

# Discriminative estimated cumulants-based automatic modulation classification over multipath fading channels

Iyad Kadoun

malek-ashtar university of technology

Hossein Khaleghi Bizaki (✉ [bizaki@yahoo.com](mailto:bizaki@yahoo.com))

Electrical and Electronic Engineering University Complex <https://orcid.org/0000-0001-9458-8287>

---

## Research Article

**Keywords:** Automatic Modulation Classification, Higher-order Cumulants, Multipath fading channel, Feature selection algorithms

**Posted Date:** July 28th, 2022



**DOI:** <https://doi.org/10.21203/rs.3.rs-1867152/v1>

**License:**  This work is licensed under a Creative Commons Attribution 4.0 International License.

[Read Full License](#)

---

# Discriminative estimated cumulants-based automatic modulation classification over multipath fading channels

Iyad Kadoun<sup>1</sup> , Hossein Khaleghi Bizaki<sup>1\*</sup> 

<sup>1</sup> Electrical and Computer Engineering Department, Malek Ashtar University of Technology, Tehran, Iran

\*[bizaki@yahoo.com](mailto:bizaki@yahoo.com)

**Abstract:** Automatic modulation classification (AMC) is an essential task in intelligent receivers. AMC research papers over multipath fading channels have two problems. The first problem is the Higher-order moment (HOM)-based normalized channel coefficients estimator is not valid for some types of digital modulations. The second problem is poor classification accuracy. This paper solves these problems through significant steps, first, by finding a new HOM-based normalized channel coefficients estimator for all cases of digital modulation types, and second, by finding the mathematical forms of the transmitted signal's estimated normalized HOMs and Higher-order cumulants (HOCs), and third, by selecting the most discriminative estimated HOCs for AMC using features selection algorithms. The simulation results show that the classification accuracy of the selected estimated HOCs, for M-array Phase Shift Keying (MPSK) and M-array quadrature amplitude shift modulation (MQAM) classification is highly improved compared with reference papers. It's 100% for the three-tap multipath channel case, and Signal-to-noise ratio (SNR) values greater than 6 dB.

**Keywords** Automatic Modulation Classification, Higher-order Cumulants, Multipath fading channel, Feature selection algorithms.

## 1 Introduction

The automatic modulation classification (AMC) algorithm determines the modulation type of the received signal. This task is somehow simple over the Additive white Gaussian noise (AWGN) channel, but it becomes more complicated over the multipath fading channel.

Research papers [1-3] improved the AMC performance using HOCs over AWGN channels. Our work focuses on improving the AMC performance using HOCs but over multipath fading channels. Research papers classify the digital modulation types over multipath fading channels through two steps [4-6]: First, the normalized channel coefficients are estimated using the HOM of the received signal. Second, some of the normalized cumulants of the transmitted signal are estimated based on the previously estimated normalized coefficients.

In [4], the author shows the performance accuracy of binary phase-shift keying (BPSK) and Quadrature Phase-Shift Keying (QPSK) classification, using the estimated normalized cumulant  $\hat{C}_{42,x}$  of the transmitted signal for the four-tap multipath case and SNR value of 10 dB is 89%. The performance accuracy of 4-quadrature amplitude modulation (4QAM), 16QAM, and 64QAM classification is 77%. In [5], the author shows the performance accuracy of BPSK and QPSK classification, using the estimated normalized cumulant  $\hat{C}_{63,x}$  of the transmitted signal for the four-tap multipath case, and SNR value of 10 dB is 91%. The performance accuracy of QPSK, 16QAM, and 64QAM classification is 45%. In [6], the author shows the performance accuracy of BPSK, QPSK, 8PSK, 16QAM, and 64QAM classification, using three normalized estimated cumulants  $\hat{C}_{40,x}$ ,  $\hat{C}_{41,x}$ , and  $\hat{C}_{42,x}$  of the transmitted signal for the four-tap multipath case and SNR value of 10 dB is 82%. As a result, the AMC performance degrades for lower SNR values cases. So, the selected estimated HOCs in [4-6] have poor performance for AMC over the multipath fading channel.

Deep learning techniques have also been used to classify digital modulations over multipath channels [7,8]. In [7], the author uses the convolutional neural network technique (CNN) to classify PSK, QAM, frequency-shift keying (FSK), Pulse-amplitude modulation (PAM), and analog modulation. The performance accuracy for SNR value of 10 dB is 90%. In [8], the author uses  $C_{60,y}$  and  $C_{63,y}$  of the received signal as input features to the stacked convolutional auto-encoder to classify BPSK, QPSK, 16-QAM, and 64-QAM over the multipath channel. The performance accuracy for the 5-tap multipath Rayleigh fading channel and SNR value of 10 dB is 91%.

As shown in [4-8], the performance accuracy degrades as the SNR value drops because of the poor performance of the selected HOCs over the multipath fading channel, which is the first problem. Another problem is found, the existing HOM-based normalized channel coefficients estimator in [4-6] can't be used for some digital modulation types like 8PSK and 16PSK (this problem will be explained in Section 3). so, the cumulants can't be estimated based on it, and modulation classification can't be done.

The significant contribution of this paper is to solve these problems through four steps: First, finding a new HOM-based normalized channel coefficients estimator alternative to the existing one in [4-6] for more cases of digital modulation types. Second, finding the mathematical forms of the estimated normalized HOMs of the transmitted signal based on the previously estimated normalized channel coefficients. Third, finding the mathematical forms of the estimated normalized HOCs of the transmitted signal based on the previously estimated normalized HOMs. Fourth, select the most discriminative estimated HOCs for AMC using the feature selection algorithms. The simulation results show that the selected estimated HOCs have improved the classification accuracy compared with reference papers [4-6], the maximum classification accuracy improvement from the reference paper [4] is 40.73%, from the reference paper [5] is 42.99, and from the reference paper [6] is 40.21%. The performance accuracy of the selected estimated HOCs is 100% for the three-tap multipath channel and SNR values greater than 6 dB and for the four-tap multipath channel and SNR values greater than 7 dB.

The rest of this paper is organized as follows. In Section 2, we describe the related signal model and the general form of HOCs and HOMs. In Section 3, we explain the problem of the normalized channel coefficients estimator in reference papers [4-6]. In Section 4, we explain the proposed normalized channel coefficients estimator. In Section 5, we estimate the transmitted signal's normalized HOMs. In Section 6, we estimate the transmitted signal's normalized HOCs. In Section 7, we apply feature selection algorithms to get on the best estimated HOCs for AMC. In Section 8, we compare the performance of the selected estimated HOCs in reference papers [4-6] with our selected estimated HOCs for AMC. Finally, we conclude this paper in Section 9.

## 2 System model

The mathematical form of the received signal over a multipath fading channel can be written as:

$$y(n) = \sum_{k=0}^{L-1} h(k)x(n-k) + w(n) := r(n) + w(n) \quad (1)$$

where  $L$  is the number of multipath taps,  $x(n-k), k=0, \dots, L-1$  are the transmitted digital modulated symbols which are considered independent and identically distributed (i.i.d) random processes,  $h(k), k=0, \dots, L-1$  are modeled as complex channel fading coefficients as  $h(k) \in CN(0, \sigma_h^2)$ ,  $r(n)$  is the noise-free received signal, and  $w(n)$  is zero-mean complex AWGN which is considered as  $w(n) \in CN(0, N)$ .

MPSK and MQAM have been used in [4-8]. BPSK, QPSK, 8PSK, 16PSK, 8QAM, 16QAM, 32QAM, and 64QAM have been chosen for this paper. As shown in Section 1, the estimated normalized HOCs have been used for AMC over the multipath channel. First, we define HOMs of the received signal  $y(n)$  as [6]:

$$M_{pq} = E[y(k)^{p-q} y^*(k)^q] \quad (2)$$

where  $*$  denotes the complex conjugate,  $p$  is the order of the moment, and  $q$  is the complex conjugate order of the moment.

Second, we define HOCs of the received signal  $y(n)$  as [6]:

$$C_{pq} = \text{Cum}[\underbrace{y_1, \dots, y_{p-q}}_{p-q \text{ terms}}, \underbrace{y_{p-q+1}^*, \dots, y_p^*}_{q \text{ terms}}] \quad (3)$$

where  $p$  is the order of the cumulant,  $q$  is the complex conjugate order of the cumulant, and  $\text{cum}$  function is defined as [9]:

$$\text{Cum}[y_1, \dots, y_n] = \sum_{\mathbf{v}} (-1)^{q-1} (q-1)! E[\prod_{j \in V_1} y_j] \dots E[\prod_{j \in V_q} y_j] \quad (4)$$

where the sum is being performed over all partitions  $V = (V_1, V_2, \dots, V_q)$  for the set of indexes  $(1, 2, \dots, n)$ .

Two feature normalizations are necessary. The first normalization is to avoid the effect of the signal's power level on the values of the features, as shown in Eq. (5) [5,10]. The second normalization is to reduce the range of the values of the feature for different digital modulation types, as shown in Eq. (6) [11,12]:

$$M'_{pq} = \frac{M_{pq}}{(M_{21})^{p/2}}, C'_{pq} = \frac{C_{pq}}{(C_{21})^{p/2}} \quad (5)$$

$$M''_{pq} = (M'_{pq})^{2/p}, C''_{pq} = (C'_{pq})^{2/p} \quad (6)$$

### 3 The HOM-based normalized channel coefficients estimator problem

Research papers like [4-6] use the  $M_{40,y}$  moment of the received signal to estimate the normalized channel coefficients as follows [4-6]:

I. The mathematical form of the joint  $M_{40,y}$  (moment with different time delays) is written as:

$$M_{40,y}(\tau, \sigma, \theta) = E[y(n)y(n+\tau)y(n+\sigma)y(n+\theta)] \quad (7)$$

where  $\tau, \sigma$ , and  $\theta$  represent three-time delays [6].

II. Since transmitted symbols  $x(n)$  are considered i.i.d,  $x(n)$  satisfies [6]:

$$E[x(n)x(n+\tau)x(n+\sigma)x(n+\theta)] = \begin{cases} M_{40,x}, & \tau = \sigma = \theta \\ 0, & \text{otherwise} \end{cases} \quad (8)$$

III. HOMs of  $w(n)$  noise signal in Eq. (1) are calculated as[13]:

$$E[w^k(n)] = 0, k = 1, 2, \dots, E[w^k(n)w^{*l}(n)] = \begin{cases} k!N^k & \text{if } k = l \\ 0 & \text{if } k \neq l \end{cases} \quad (9)$$

where  $N$  is the noise power.

IV. Substituting the mathematical form of the received signal  $y(n)$  Eq. (1), Eqs. (8), and (9) into Eq. (7), for desired time delays of  $\tau, \sigma, \theta$ , we find:

$$M_{40,y}(\tau, \sigma, \theta) = M_{40,x} \sum_{k=0}^{L-1} h(k)h(k+\tau)h(k+\sigma)h(k+\theta) \quad (10)$$

V. To estimate the normalized channel coefficients, the moment  $M_{40,y}$  in Eq. (10) is calculated for two cases:  $\{\tau = 0, \sigma = \theta = L-1\}$  and  $\{\tau = k, \sigma = \theta = L-1\}$  as [6]:

$$M_{40,y}(0, L-1, L-1) = M_{40,x} h(0)h(0)h(L-1)h(L-1) \quad (11)$$

$$M_{40,y}(k, L-1, L-1) = M_{40,x} h(k)h(k)h(L-1)h(L-1) \quad (12)$$

where  $0 \leq k \leq L-1$ .

VI. Dividing Eq. (11) by Eq. (12) under the nonzero condition  $M_{40,x} \neq 0$ , the normalized multipath channel coefficients are estimated as [6]:

$$\hat{h}(k) = \frac{h(k)}{h(0)} = \frac{M_{40,y}(k, L-1, L-1)}{M_{40,y}(0, L-1, L-1)}, 0 \leq k \leq L-1 \quad (13)$$

The normalized channel coefficients can be estimated by calculating the joint moments  $M_{40,y}(k, L-1, L-1)$  and  $M_{40,y}(0, L-1, L-1)$  of the received signal  $y(n)$  in Eq. (13). We briefly call the  $M_{40}$ -based normalized channel coefficients estimator  $M_{40}$ -NCCE. Unfortunately, condition  $M_{40,x} \neq 0$  is not satisfied for some of the selected digital modulation types in Section 2, like 8PSK and 16PSK, as shown in Table 2 in [14] and Table 1 in [15]. Hence, this estimator can't be used in the case of these modulation types.

As a result, to classify the chosen digital modulation types in Section 2,  $M_{40}$ -NCCE can't be used. A new alternative estimator must be found under the nonzero moment condition for all cases of digital modulation types. The main steps of AMC improvement over the multipath channel are shown in Fig. 1.

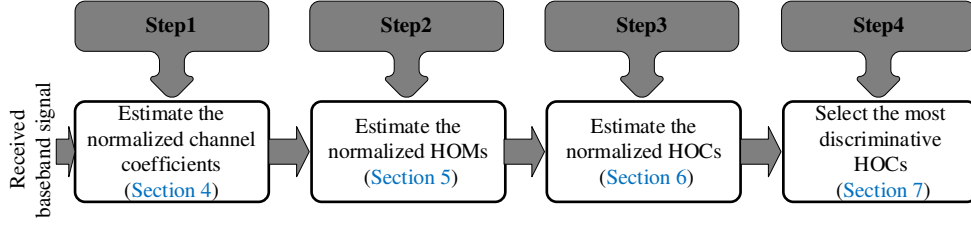


**Fig. 1** The main steps of the AMC improvement over multipath fading channels

Fig. 1 shows four main steps for AMC improvement over multipath fading channels. Step1 is finding a new HOM-based normalized channel coefficients estimator alternative to the existing one in [4-6] for the selected digital modulation types in Section 2, as shown in Section 4. Step2 is finding the mathematical forms of the estimated normalized HOMs of the transmitted signal based on the previously estimated normalized channel coefficients, as shown in Section 5. Step3 is finding the mathematical forms of the estimated normalized HOCs of the transmitted signal based on the previously estimated normalized HOMs, as shown in Section 6. Step4 is selecting the most discriminative HOCs for AMC using the feature selection algorithms, as shown in Section 7.

#### 4 The proposed HOM-based normalized channel coefficients estimator (step1)

##### 4.1 The proposed channel coefficients estimator

Looking at Table 2 in [14] and Table 1 in [15], the value  $M_{42,x} \neq 0$  for all digital modulations because of  $|x(n)|^4 > 0, \forall x(n) \neq 0$ , so we can use it to estimate the channel coefficients as follows:

I. Calculate the moment  $M_{42,y}(\tau, \sigma, \theta)$  using Eq. (1) as:

$$\begin{aligned}
 M_{42,y}(\tau, \sigma, \theta) &= E[y(n)y(n+\tau)y^*(n+\sigma)y^*(n+\theta)] \\
 &= E[(r(n)+w(n))(r(n+\tau)+w(n))(r^*(n+\sigma)+w^*(n))(r^*(n+\theta)+w^*(n))] \\
 &= E[r(n)r(n+\tau)r^*(n+\sigma)r^*(n+\theta)] + (M_{21,r}(\sigma) + M_{21,r}(\theta) + M_{21,r}(\sigma-\tau) + M_{21,r}(\theta-\tau))N + 2N^2
 \end{aligned} \tag{14}$$

where  $\tau, \sigma$ , and  $\theta$  represent three-time delays.

II. Calculate  $M_{21,r}$  as:

$$\begin{aligned}
 M_{21,y}(\xi) &= E[y(n)y^*(n+\xi)] = M_{21,r}(\xi) + N \\
 \Rightarrow M_{21,r}(\xi) &= M_{21,y}(\xi) - N
 \end{aligned} \tag{15}$$

where  $\xi$  is a time delay.

III. Substitute Eq. (15) into Eq. (14) and use Eq. (9) to obtain:

$$\begin{aligned}
 M_{42,y}(\tau, \sigma, \theta) &= \\
 &= E[r(n)r(n+\tau)r^*(n+\sigma)r^*(n+\theta)] + (M_{21,y}(\sigma) + M_{21,y}(\theta) + M_{21,y}(\sigma-\tau) + M_{21,y}(\theta-\tau))N - 2N^2
 \end{aligned} \tag{16}$$

IV. To estimate the normalized channel coefficients, we calculate the joint moment  $M_{42,y}$  Eq. (16) for two cases:  $\{\tau=0, \sigma=0, \theta=L-1\}$  and  $\{\tau=0, \sigma=k, \theta=L-1\}$  as:

$$\begin{aligned}
 M_{42,y}(0, k, L-1) &= h(0)^2 h^*(L-1) h^*(k) M_{42,x} + 2(M_{21,y}(k) + M_{21,y}(L-1))N - 2N^2 \\
 \Rightarrow h(0)^2 h^*(L-1) h^*(k) M_{42,x} &= M_{42,y}(0, k, L-1) - 2(M_{21,y}(k) + M_{21,y}(L-1))N + 2N^2
 \end{aligned} \tag{17}$$

$$\begin{aligned}
 M_{42,y}(0, 0, L-1) &= h(0)^2 h^*(L-1) h^*(0) M_{42,x} + 2(M_{21,y}(L-1) + M_{21,y})N - 2N^2 \\
 \Rightarrow h(0)^2 h^*(L-1) h^*(0) M_{42,x} &= M_{42,y}(0, 0, L-1) - 2(M_{21,y}(L-1) + M_{21,y})N + 2N^2
 \end{aligned} \tag{18}$$

where  $0 \leq k \leq L-1$ .

V. Since  $M_{42,x} \neq 0$  for all mentioned digital modulation types, divide Eq. (17) by Eq. (18) to get on the new normalized channel coefficients estimator as:

$$\hat{h}(k) = \frac{h(k)}{h(0)} = \left( \frac{M_{42,y}(0, k, L-1) - 2(M_{21,y}(L-1) + M_{21,y}(k))N + 2N^2}{M_{42,y}(0, 0, L-1) - 2(M_{21,y}(L-1) + M_{21,y})N + 2N^2} \right)^* , 0 \leq k \leq L-1 \tag{19}$$

The normalized channel coefficients can be estimated by calculating the joint moments  $M_{42,y}(0,k,L-1)$ ,  $M_{42,y}(0,0,L-1)$ ,  $M_{21,y}(L-1)$ ,  $M_{21,y}(k)$ , and  $M_{21,y}$  of the received signal  $y(n)$  in Eq. (19). We briefly call the  $M_{42}$ -based normalized channel coefficients estimator  $M_{42}$ -NCCE.

#### 4.2 Comparison between the performance of $M_{40}$ -NCCE and $M_{42}$ -NCCE

As we have mentioned in Section 3,  $M_{40}$ -NCCE can't be used for the classification problem of the mentioned modulations. To check the performance of our proposed  $M_{42}$ -NCCE, a comparison between the performance of  $M_{42}$ -NCCE in Eq. (19) and  $M_{40}$ -NCCE in Eq. (13) has been done for the four-tap multipath channel case as follows:

- I. Choose the digital modulation types under the nonzero condition  $M_{40,x} \neq 0$  (so the  $M_{40}$ -NCCE is valid), like BPSK, QPSK, 16QAM, and 64QAM.
- II. Estimate the normalized channel coefficients using  $M_{40}$ -NCCE in Eq. (13) and  $M_{42}$ -NCCE in Eq. (19).
- III. Using the previously estimated normalized coefficients, estimate the normalized  $\hat{C}_{42,x}$  according to its mathematical form in reference papers [4,6] and  $\hat{C}_{63,x}$  according to its mathematical form in reference paper [5].
- IV. Calculate their second normalization  $\tilde{C}_{42,x}$  and  $\tilde{C}_{63,x}$  according to Eq. (6).
- V. Calculate  $E(\tilde{C}_{42,x})$  and  $E(|\tilde{C}_{42,x} - C_{42,x}|^2)$  for the selected digital modulation types in step1, as shown in Fig. 2, and calculate  $E(\tilde{C}_{63,x})$  and  $E(|\tilde{C}_{63,x} - C_{63,x}|^2)$ , as shown in Fig. 3, where  $C_{42,x}$  and  $C_{63,x}$  are the theoretical values of the normalized cumulants.

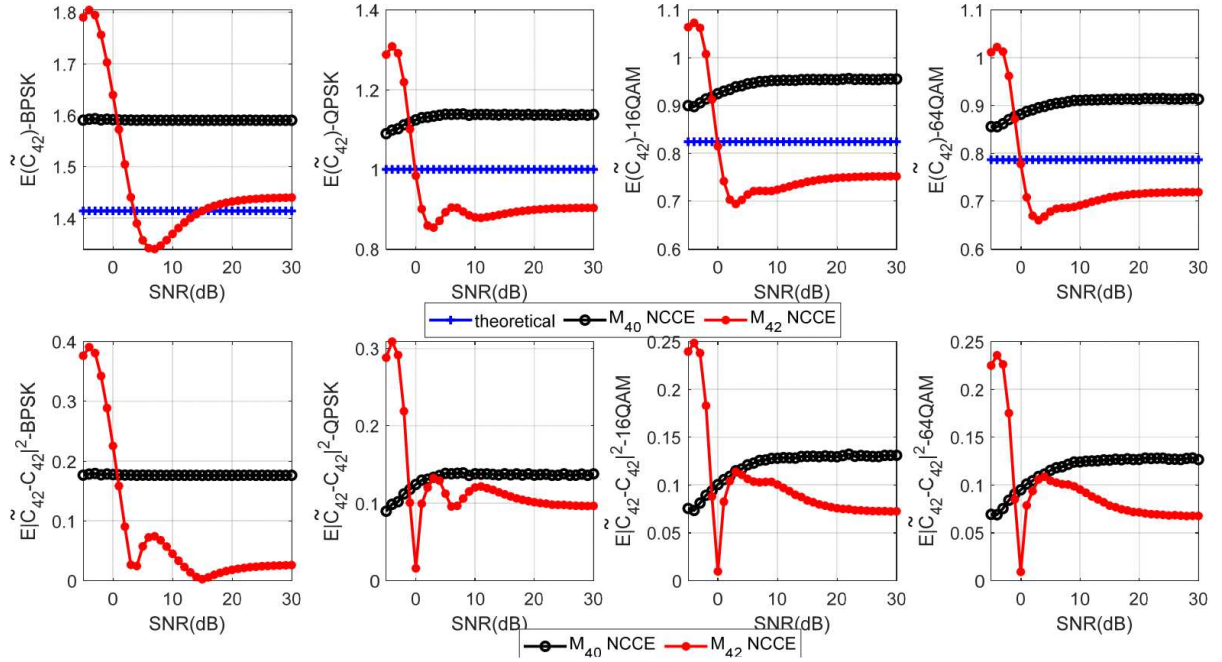


**Fig. 2** Values of  $E(\tilde{C}_{42,x})$  and  $E(|\tilde{C}_{42,x} - C_{42,x}|^2)$  based on  $M_{40}$ -NCCE and  $M_{42}$ -NCCE channel coefficients estimators for BPSK, QPSK, 16QAM, and 64QAM digital modulation types



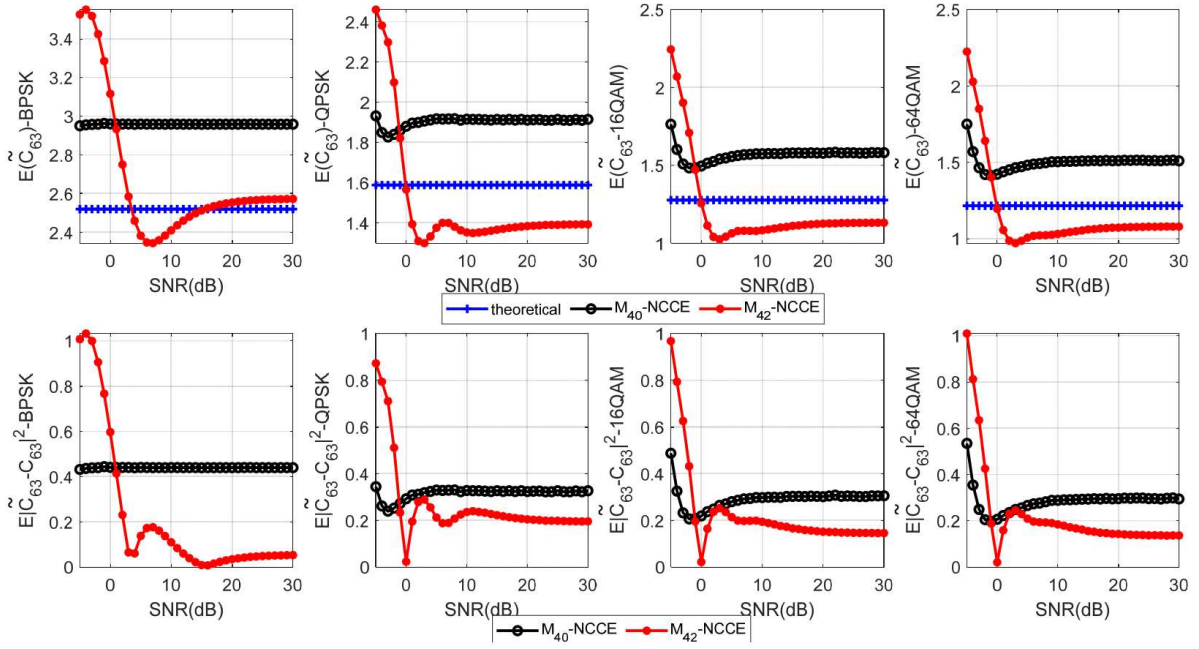


**Fig. 3** Values of  $E(\tilde{C}_{63,x})$  and  $E(|\tilde{C}_{63,x} - C_{63,x}|^2)$  based on  $M_{40}$ -NCCE and  $M_{42}$ -NCCE channel coefficients estimators for BPSK, QPSK, 16QAM, and 64QAM digital modulation types

As shown in Figs. 2 and 3,  $E(\tilde{C}_{42,x})$  and  $E(\tilde{C}_{63,x})$  are closer to their theoretical values (for SNR values greater than -2 dB) by using the  $M_{42}$ -NCCE-based estimated normalized channel coefficients. As a result,  $M_{42}$ -NCCE has better performance than  $M_{40}$ -NCCE.

## 5 The proposed estimators of the transmitted signal's normalized HOMs (step2)

### 5.1 The proposed HOMs estimators

Since the normalized channel coefficients have been estimated using the new estimator  $M_{42}$ -NCCE in Section 4, the normalized HOMs in Eq. (5) can be estimated based on it. To estimate the normalized HOMs, i.e.,  $\hat{M}_{20,x}$  in Eq. (5),  $M_{20,x}$  and  $M_{21,x}$  should be calculated first as:

- I. Calculate the relationship between the HOMs of the received signal  $y(n)$  ( $M_{20,y}, M_{21,y}$ ) and the HOMs of the noise-free received signal  $r(n)$  ( $M_{20,r}, M_{21,r}$ ) in Eq. (1) using Eq. (9) for  $M_{20,y}$  and  $M_{21,y}$  as:

$$M_{20,y} = M_{20,r}, \quad M_{21,y} = M_{21,r} + N \Rightarrow M_{21,r} = M_{21,y} - N \quad (20)$$

- II. Calculate  $M_{20,r}$  and  $M_{21,r}$  by using the estimated normalized channel coefficients, then calculate  $M_{20,x}$  and  $M_{21,x}$  by using Eq. (20) as:

$$M_{20,r} = h(0)^2 \alpha_{20} M_{20,x} \Rightarrow M_{20,x} = \frac{M_{20,r}}{h(0)^2 \alpha_{20}} = \frac{M_{20,y}}{h(0)^2 \alpha_{20}}, \text{ where } \alpha_{20} = \sum_{k=0}^{L-1} \hat{h}(k)^2 \quad (21)$$

$$M_{21,r} = |h(0)|^2 \alpha_{21} M_{21,x} \Rightarrow M_{21,x} = \frac{M_{21,r}}{|h(0)|^2 \alpha_{21}} = \frac{M_{21,y} - N}{|h(0)|^2 \alpha_{21}}, \text{ where } \alpha_{21} = \sum_{k=0}^{L-1} |\hat{h}(k)|^2$$

- III. Calculate the estimated normalized  $M_{20,x}$  using Eqs. (21) and (5) as:

$$\hat{M}_{20,x} = \frac{M_{20,x}}{M_{21,x}} = \frac{h(0)^* \alpha_{21}}{h(0) \alpha_{20}} \frac{M_{20,y}}{M_{21,y} - N} := \frac{h(0)^*}{h(0)} \hat{m}_{20,x}, \quad \hat{m}_{20,x} = \frac{\alpha_{21}}{\alpha_{20}} \frac{M_{20,y}}{M_{21,y} - N} \quad (22)$$

where  $M_{20,y}$  and  $M_{21,y}$  are 2<sup>nd</sup> order moments of the received signal  $y(n)$ ,  $\alpha_{21}$  and  $\alpha_{20}$  are calculated by using the estimated normalized coefficients in Eq. (19). Only one unknown parameter, i.e.,  $h(0)^* / h(0)$ , can be obtained by

calculating its absolute value:  $|h(0)^*|/|h(0)|=1 \Rightarrow |\hat{M}_{20,x}|=|\hat{m}_{20,x}|$ .

For the estimated normalized  $\tilde{M}_{21,x}$ , its value is equal to 1 according to Eq. (5) ( $\tilde{M}_{21,x} = \tilde{m}_{21,x} = 1$ ). Like  $M_{20,x}$ , all other moments can be estimated. Starting with step1 in this Section, Table 1 shows the relationship between the HOMs of the received signal  $y(n)$  and the HOMs of the noise-free received signal  $r(n)$  of Eq. (1):

**Table 1** The relationship between the HOMs of the received signal  $y(n)$  and the HOMs of the noise-free received signal  $r(n)$  of Eq. (1)

$M_{40,y} = M_{40,r}$	(23)
$M_{41,y} = M_{41,r} + 3M_{20,y}N$	(24)
$M_{42,y} = M_{42,r} + 4M_{21,r}N + 2N^2$	(25)
$M_{60,y} = M_{60,r}$	(26)
$M_{61,y} = M_{61,r} + 5M_{40,r}N = M_{61,r} + 5M_{40,y}N$	(27)
$M_{62,y} = M_{62,r} + 8M_{41,r}N + 12M_{20,r}N^2 = M_{62,r} + 8M_{41,y}N - 12M_{20,y}N^2$	(28)
$M_{63,y} = M_{63,r} + 9M_{42,r}N + 18M_{21,r}N^2 = M_{63,r} + 9M_{42,y}N - 18M_{21,y}N^2$	(29)
$M_{80,y} = M_{80,r}$	(30)
$M_{81,y} = M_{81,r} + 7M_{60,r}N = M_{81,r} + 7M_{60,y}N$	(31)
$M_{82,y} = M_{82,r} + 12M_{61,r}N + 26M_{40,r}N^2 = M_{82,r} + 12M_{61,y}N - 34M_{40,y}N^2$	(32)
$M_{83,y} = M_{83,r} + 15M_{62,r}N + 60M_{41,r}N^2 + 60M_{20,r}N^3 = M_{83,r} + 15M_{62,y}N - 60M_{41,y}N^2 + 60M_{20,y}N^3$	(33)
$M_{84,y} = M_{84,r} + 16M_{63,r}N + 72M_{42,r}N^2 + 96M_{21,r}N^3 + 72N^4$ $= M_{84,r} + 16M_{63,y}N - 72M_{42,y}N^2 + 96M_{21,y}N^3 + 72N^4$	(34)

We continue calculating the estimated normalized HOMs in steps 2 and 3. Appendix 1 summarizes the mathematical forms of the estimated normalized HOMs without any approximation.

## 5.2 Validation of HOMs estimators

To validate the HOMs estimators, calculation of  $\hat{M}_{pq,x}$  (in Appendix 1) and  $|\tilde{M}_{pq,x}|$  (in Eq. (6)) is done for the case of BPSK modulation (as an example) under perfect channel coefficients. Comparisons with their theoretical values are shown in Fig. 4 for the four-tap multipath channel case.



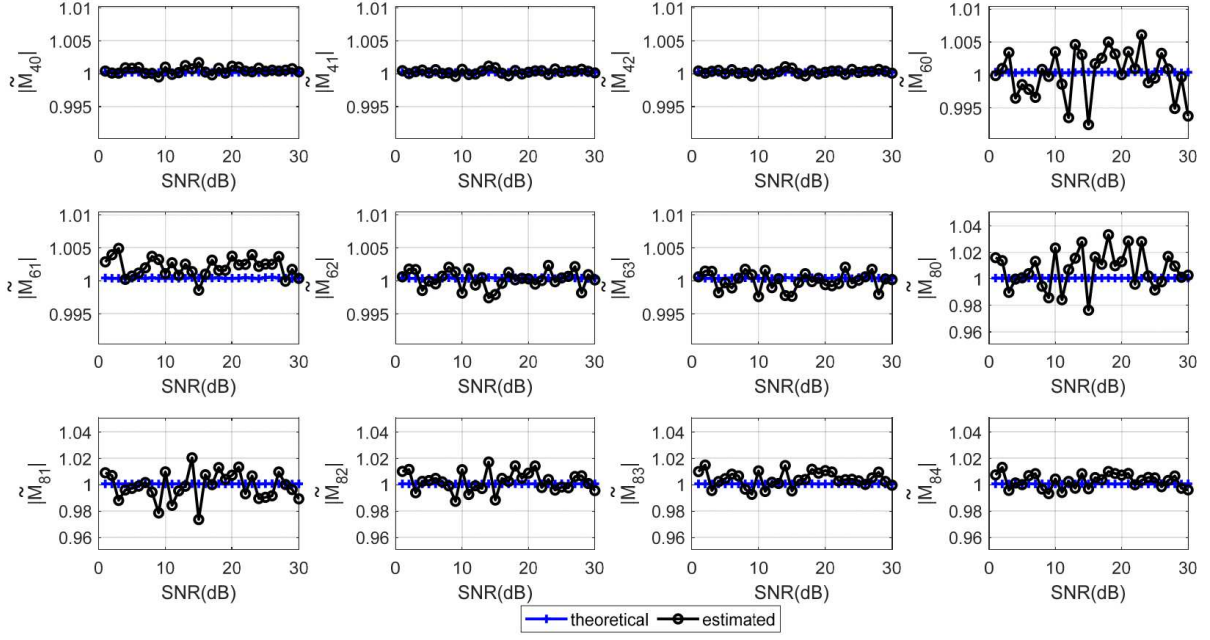


**Fig. 4** The values of the theoretical and the estimated normalized HOMs of BPSK modulation under perfect channel coefficients

As shown in Fig. 4, the estimated HOMs are similar to their theoretical values, so the mathematical forms are confirmed.

## 6 The proposed estimators of the transmitted signal's normalized HOCs (step3)

### 6.1 The proposed HOCs estimators

After HOMs have been estimated, the normalized HOCs can be estimated using the estimated HOMs in Section 5 based on the equations in Table 2 [16-20]:

**Table 2** Mathematical relationships between HOMs and HOCs

$C_{20} = M_{20}$	(35)
$C_{21} = M_{21}$	(36)
$C_{40} = M_{40} - 3M_{20}^2$	(37)
$C_{41} = M_{41} - 3M_{20}M_{21}$	(38)
$C_{42} = M_{42} -  M_{20} ^2 - 2M_{21}^2$	(39)
$C_{60} = M_{60} - 15M_{20}M_{40} + 30M_{20}^3$	(40)
$C_{61} = M_{61} - 5M_{21}M_{40} - 10M_{20}M_{41} + 30M_{20}^2M_{21}$	(41)
$C_{62} = M_{62} - 6M_{20}M_{42} - 8M_{21}M_{41} - M_{22}M_{40} + 6M_{20}^2M_{22} + 24M_{21}^2M_{22}$	(42)
$C_{63} = M_{63} - 9M_{21}M_{42} + 12M_{21}^3 - 3M_{20}M_{43} - 3M_{22}M_{41} + 18M_{20}M_{21}M_{22}$	(43)
$C_{80} = M_{80} - 35M_{40}^2 - 28M_{60}M_{20} + 420M_{20}^2M_{40} - 630M_{20}^4$	(44)
$C_{81} = M_{81} - 7M_{60}M_{21} - 21M_{61}M_{20} - 35M_{40}M_{41} + 210M_{40}M_{20}M_{21} + 210M_{20}^2M_{41} - 630M_{20}^3M_{21}$	(45)
$C_{82} = M_{82} - M_{60}M_{22} - 12M_{61}M_{21} - 15M_{62}M_{20} - 15M_{40}M_{42} + 30M_{40}M_{20}M_{22} + 60M_{40}M_{21}^2$ $- 20M_{41}^2 + 240M_{41}M_{20}M_{21} + 90M_{42}M_{20}^2 - 90M_{20}^3M_{22} - 540M_{20}^2M_{21}^2$	(46)

$$C_{83} = M_{83} - 3M_{61}M_{22} - 15M_{62}M_{21} - 5M_{40}M_{43} + 30M_{40}M_{21}M_{22} - 10M_{63}M_{20} - 30M_{41}M_{42} \quad (47)$$

$$+ 60M_{41}M_{20}M_{22} + 120M_{41}M_{21}^2 + 30M_{20}^2M_{43} - 270M_{20}^2M_{21}M_{22} - 360M_{20}M_{21}^3 + 180M_{20}M_{42}M_{21}$$

$$C_{84} = M_{84} - 16C_{63}C_{21} + |C_{40}|^2 - 18C_{42}^2 - 72C_{42}C_{21}^2 - 24C_{21}^4 \quad (48)$$

The remaining HOCs in [Table 2](#) are calculated using [Eq. \(2\)](#) as  $M_{p,q} = M_{p,p-q}^*$ , as an example,  $M_{22} = M_{20}^*$ ,  $M_{43} = M_{41}^*$ , and  $M_{44} = M_{40}^*$ .

Start with  $C_{40}$ , to estimate its normalized form of [Eq. \(5\)](#). Many steps should be done as follows:

- I. Calculate its normalized value [Eq. \(5\)](#) using [Eqs. \(36\)](#) and [\(37\)](#) as:

$$\hat{C}_{40} = \frac{C_{40}}{C_{21}^2} = \frac{M_{40}}{M_{21}^2} - 3\frac{M_{20}^2}{M_{21}^2} = \hat{M}_{40} - 3\hat{M}_{20}^2 \quad (49)$$

- II. Use the mathematical forms of the estimated normalized HOM [Eq. \(22\)](#) in the previous Section and [Eq. \(54\)](#) in [Appendix 1](#) as:

$$\hat{C}_{40} = \frac{h(0)^{*2}}{h(0)^2} \hat{m}_{40,x} - 3\left(\frac{h(0)^*}{h(0)} \hat{m}_{20,x}\right)^2 = \frac{h(0)^{*2}}{h(0)^2} (\hat{m}_{40,x} - 3\hat{m}_{20,x}^2) := \frac{h(0)^{*2}}{h(0)^2} \hat{c}_{40} \quad (50)$$

Only one unknown parameter  $h(0)^{*2} / h(0)^2$  can be obtained by calculating its absolute value as  $|\hat{C}_{40}| = |\hat{c}_{40}|$ .

Like  $\hat{C}_{40}$ , all remaining HOCs can be estimated. [Appendix 2](#) summarizes the mathematical forms of the estimated normalized HOCs without any approximation.

## 6.2 Validation of HOCs estimators

To validate the HOCs estimators, calculation of  $\hat{C}_{pq,x}$  (in [Appendix 2](#)) and  $|\tilde{C}_{pq,x}|$  (in [Eq. \(6\)](#)) is done for the case of BPSK modulation (as an example) under perfect channel coefficients. Comparisons with their theoretical values are shown in [Fig. 5](#) for the four-tap multipath channel case.

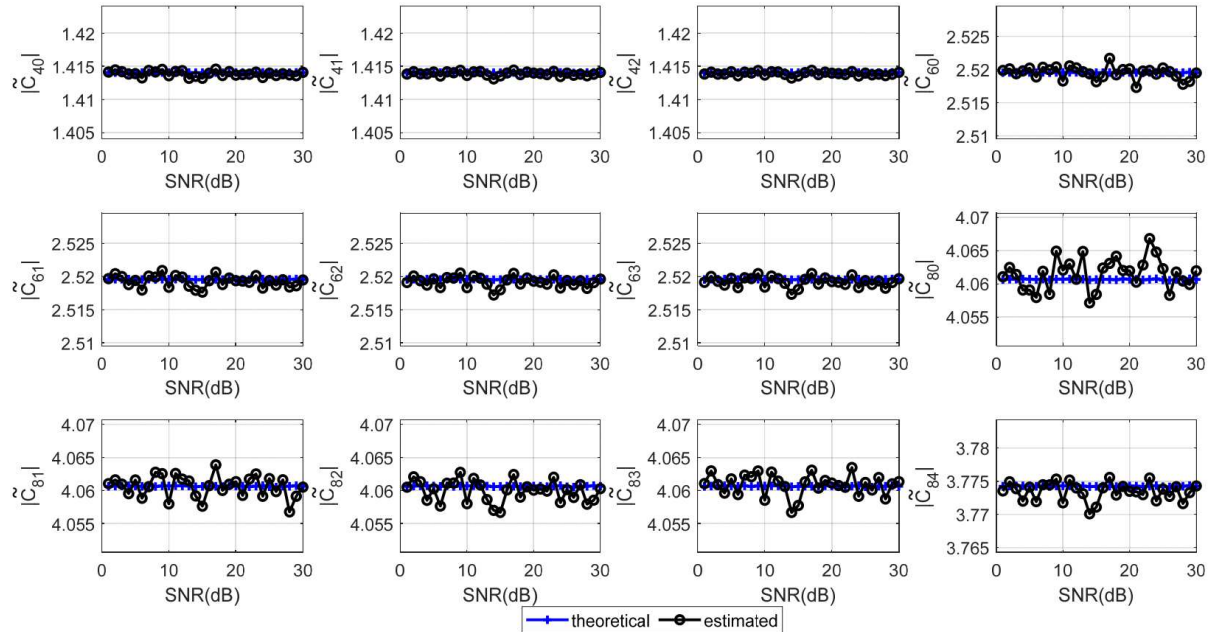


**Fig. 5** The values of the theoretical and the estimated normalized HOCs of BPSK modulation under perfect channel coefficients

As shown in Fig. 5, the estimated HOCs are similar to their theoretical values, so the mathematical forms are confirmed.

## 7 The most discriminative estimated HOCs (step4)

### 7.1 Feature selection algorithms

As shown in Section 1, the selected HOCs in [4-6] have poor classification accuracy for AMC over multipath fading channels. The most discriminative HOCs must be chosen to get the best classification accuracy. These HOCs are chosen using Feature selection algorithms. The feature selection algorithms evaluate the score of each feature according to its discrimination ability and select the features with the highest scores. As a result, they minimize the complexity, reduce the storage size, improve the learning performance, and speed up the learning process [20-22].

This paper uses two feature selection algorithms: Relief-F and Pearson correlation coefficient algorithms.

Relief-F algorithm[20,21]: is an iterative approach that estimates the score of each feature according to the differentiation of data samples that are near to each other. For each point  $i$  of class  $l$ , i.e.  $\mathbf{x}_{i,l}$ , we define  $NH(i)$  are the nearest data of  $\mathbf{x}_i$  in the same class with size  $h_i$ ,  $NM(i,k)$  are the nearest data of  $\mathbf{x}_i$  in class  $k$  ( $k \neq l$ ) with size  $h_{ik}$  and probability  $p(k)$ . The Relief-F Score can be calculated as:

$$RF(f_l) = \frac{1}{u} \sum_{i=1}^u \left( -\frac{1}{h_i} \sum_{\mathbf{x}_r \in NH(i)} d_{RF}(\mathbf{x}_{i,l}, \mathbf{x}_{r,l}) + \sum_{k \neq l} \frac{1}{h_{ik}} \frac{p(k)}{1-p(k)} \sum_{\mathbf{x}_r \in NM(i,k)} d_{RF}(\mathbf{x}_{i,l}, \mathbf{x}_{r,l}) \right) \quad (51)$$

where  $d_{RF}$  is defined as:

$$d_{RF}(\mathbf{x}_{i,l}, \mathbf{x}_{r,l}) = \begin{cases} 0 & \text{if } \mathbf{x}_{i,l} = \mathbf{x}_{r,l} \\ 1 & \text{if } \mathbf{x}_{i,l} \neq \mathbf{x}_{r,l} \end{cases} \quad (52)$$

and  $u$  is data instances are randomly selected among all  $m$  instances.

Pearson Correlation Coefficient [20,22]: measures the similarity between data samples and their labels. PCC score can be calculated as:

$$PCC(f_l) = \left| \frac{\sum_{j=1}^m (x_{j,l} - \mu_{x_l})(y_{j,l} - \mu_{y_l})}{\sqrt{\sigma_{x_l}^2 \sigma_{y_l}^2}} \right| \quad (53)$$

where  $\mu_{x_l}$  is the mean value of the feature  $l$  with variance  $\sigma_{x_l}^2$ , and  $\mu_{y_l}$  is the mean value of labels of feature  $l$  with variance  $\sigma_{y_l}^2$ .

### 7.2 Selection of the most discriminative estimated HOCs

We calculate the scores of the estimated normalized HOCs in Section 6 using relief-F and Pearson correlation coefficient algorithms and choose the highest ones. Figs. 6 and 7 show the score order of the estimated normalized HOCs.

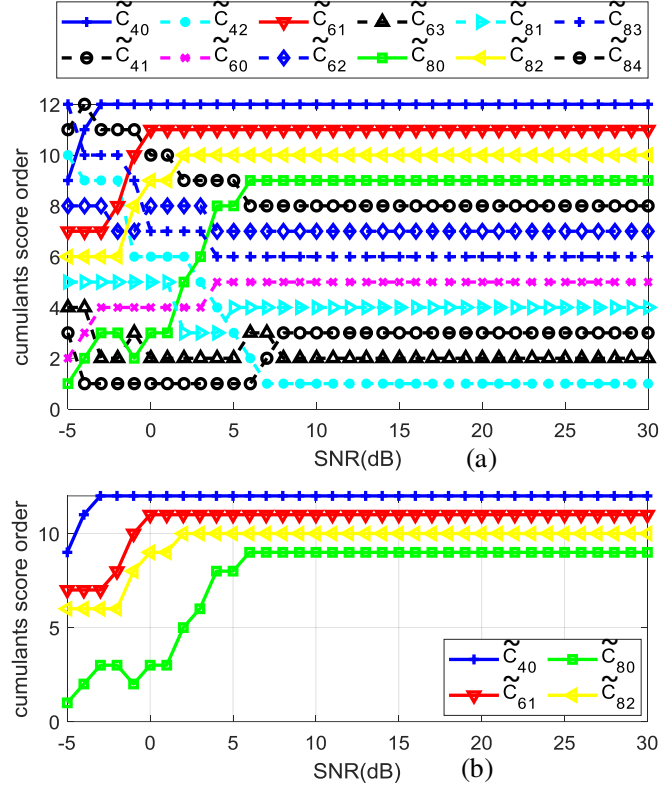


**Fig. 6** The score order of the estimated normalized HOCs based on the Relief-F algorithm

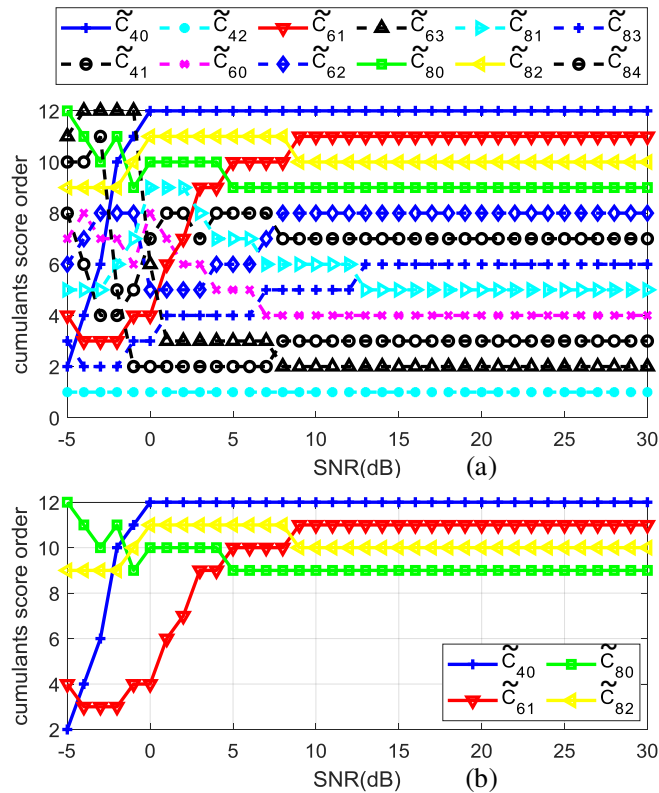


**Fig. 7** The score order of the estimated normalized HOCs based on the Pearson correlation algorithm

As shown in Figs. 6(a) and 7(a), Relief-F and Pearson correlation algorithms have four shared cumulants as the best estimated normalized cumulants  $\tilde{C}_{40}$  (continuous blue line),  $\tilde{C}_{61}$  (continuous red line),  $\tilde{C}_{80}$  (continuous green

line), and  $\tilde{C}_{82}$  (continuous yellow line). Figs. 6(b) and 7(b) show the score orders of these HOCs. According to the relief-F algorithm, these shared HOCs are the most discriminative HOCs for SNR value range [6:30] dB. And according to the Pearson correlation algorithm, these shared HOCs are the most discriminative HOCs for SNR value range [3:30] dB, so they have been chosen for the next simulation.

Figs 8, 9, 10, and 11 show the absolute values of  $\tilde{C}_{40}$  in Eq. (50),  $\tilde{C}_{61}$  ( Eq. (69) in Appendix 2),  $\tilde{C}_{80}$  ( Eq. (72) in Appendix 2), and  $\tilde{C}_{82}$  ( Eq. (74) in Appendix 2) for all SNR values.

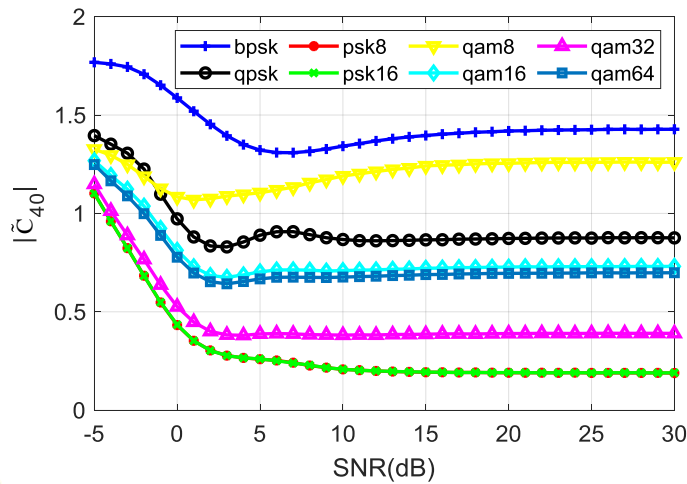


**Fig. 8** The absolute values of  $\tilde{C}_{40}$  for the selected digital modulation types in Section2 and all SNR range

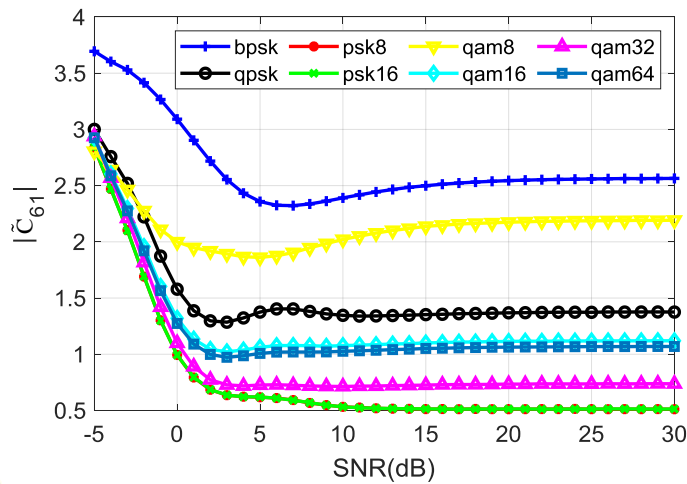


**Fig. 9** The absolute values of  $\tilde{C}_{61}$  for the selected digital modulation types in Section2 and all SNR range

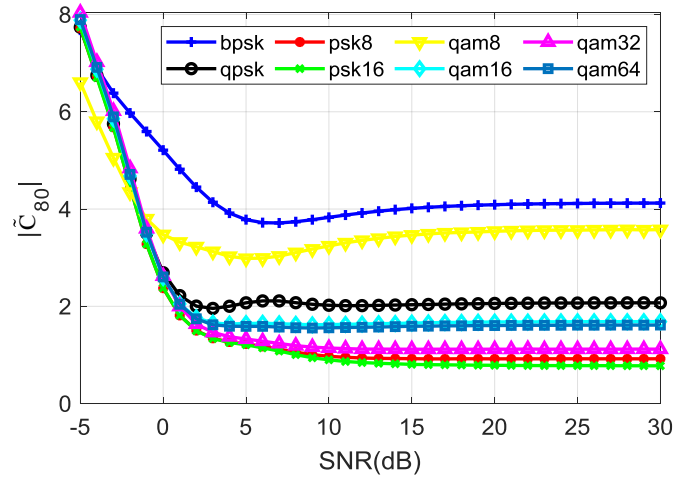


**Fig. 10** the absolute values of  $\tilde{C}_{80}$  for the selected digital modulation types in Section2 and all SNR range

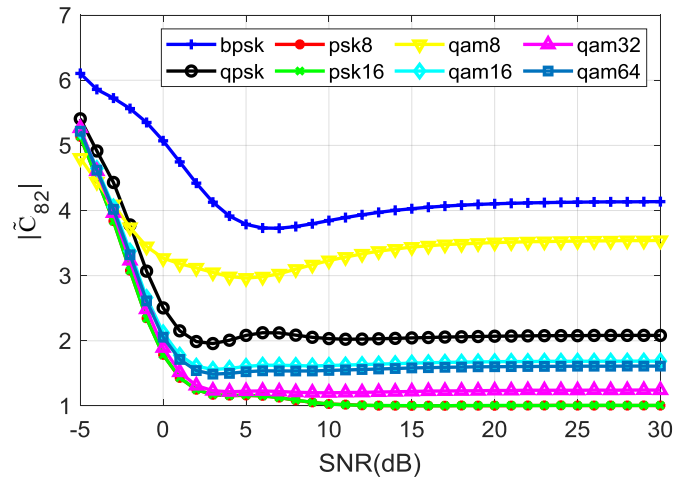


**Fig. 11** the absolute values of  $\tilde{C}_{82}$  for the selected digital modulation types in Section2 and all SNR range

Figs. 8, 9, 10, and 11 show the discrimination ability of the selected estimated HOCs  $\tilde{C}_{40}$ ,  $\tilde{C}_{61}$ ,  $\tilde{C}_{80}$ , and  $\tilde{C}_{82}$  for the selected digital modulation types in Section 2 over multipath fading channels.

The block diagram in Fig. 12 summarizes all successive stages of the most discriminative estimated HOCs selection procedure:

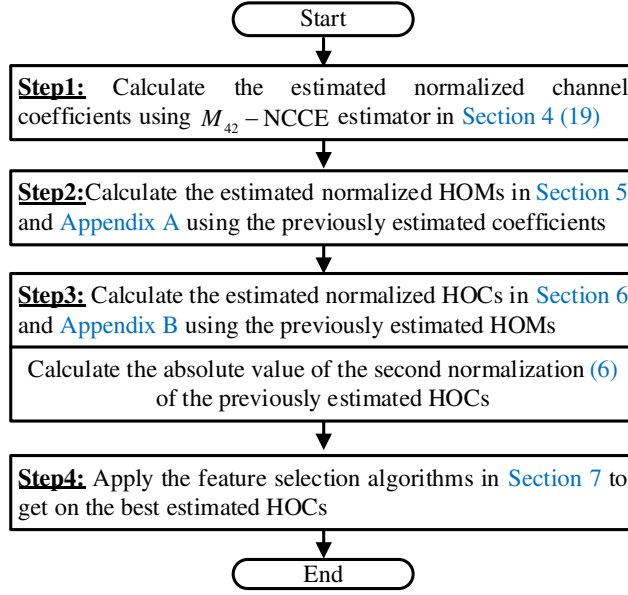


**Fig. 12** all successive stages of the most discriminative estimated HOCs selection procedure

## 8 Simulation results

The chosen Power Delay Profiles (PDP) in the simulation are [0 dB, -5 dB, -10 dB, -15 dB] have delay spread [0 symbol, 1 symbol, 2 symbols, 3 symbols] for four-taps multipath channel, and [0 dB, -4 dB, -11 dB] have delay spread [0 symbol, 1 symbol, 2 symbols] for three-taps multipath channel. The variance of the fading coefficients is  $\sigma_h^2 = 0.05$  (the same as [4-6]). Using the estimated normalized channel coefficients based on  $M_{42}$ -NCCE in Eq. (19). Two simulation stages are done to classify the proposed digital modulation types in Section 2: First, use the estimated HOCs in reference papers [4-6]. Second, use the mathematical forms (Appendix 2) of the selected estimated HOCs in Section 7.

### 8.1 Classification accuracy improvement compared with reference papers [4-6]

Fig. 13 shows the AMC performance ( $ACC^1$ ) using the estimated HOCs in reference papers [4-6] and the selected estimated HOCs in Section 7 for the 4-tap multipath case.

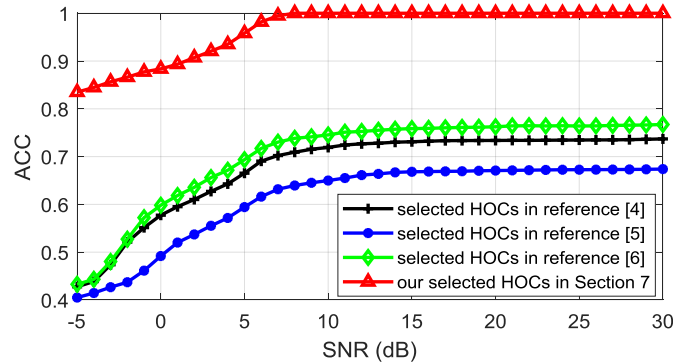


**Fig. 13** AMC performance using the estimated HOCs in reference papers [4-6] and the selected estimated HOCs in Section 7 for 4-tap multipath case

As shown in Fig. 13, the AMC performance is highly improved using the selected estimated HOCs in Section 7 compared with the reference papers [4-6].

To calculate the AMC performance improvement using the selected estimated HOCs in Section 7 compared with the reference papers [4-6]. We subtract the AMC performance of the reference papers [4-6] (blue, black, and green-

<sup>1</sup> -ACC : Classification accuracy



colored lines in Fig. 13) from the AMC performance of the selected estimated HOCs (red-colored line in Fig. 13), as shown in Fig. 14.

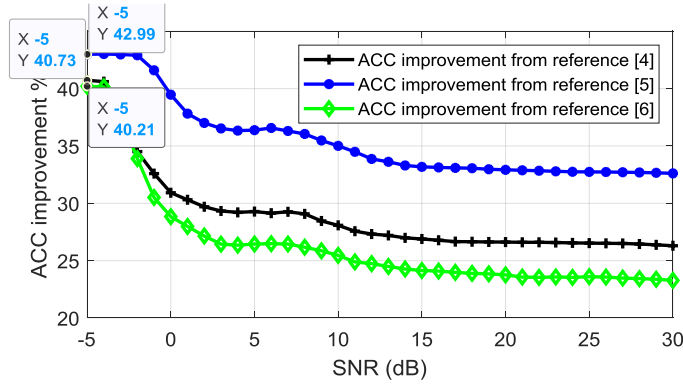


**Fig. 14.** ACC improvements using the selected HOCs in Section 7 compared with reference papers [4-6]

As shown in Fig. 14, the maximum ACC improvement from the reference paper [4] is 40.73%, from the reference paper [5] is 42.99, and from the reference paper [6] is 40.21%.

## 8.2 Classification accuracy for 3and 4-tap multipath cases

Finally, simulations of the selected HOCs for 3-tap and 4-tap multipath cases have been shown in Fig. 15.

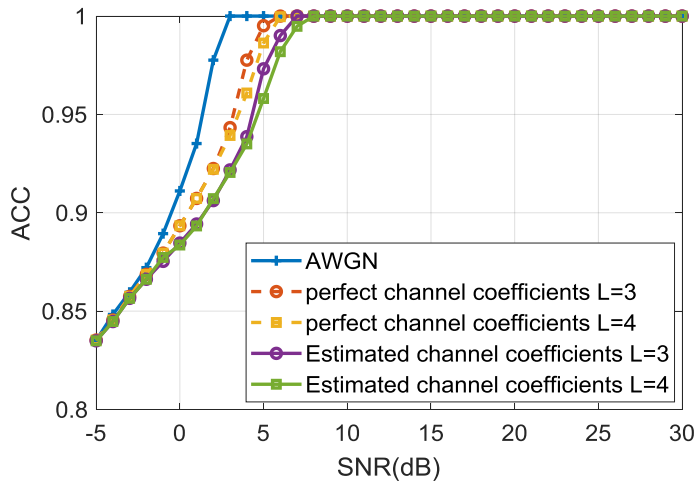


**Fig. 15** AMC Performance accuracy using the selected estimated HOCs for 3-tap and 4-tap multipath cases

As shown in Fig. 15, the simulation results show that the performance accuracy using the selected estimated HOCs in Section 7, based on the estimated channel coefficients, is 100% for the case of three-tap multipath channel and SNR values greater than 6 dB. Its performance accuracy is 100% for the case of four-tap multipath and SNR values greater than 7 dB.

## 9 Conclusion

This paper solves two existing problems in paper references [4-6] for AMC of the selected digital modulation types in Section 2 over multipath fading channels. The first problem, the normalized channel coefficients estimator  $M_{40}$ -NCCE of Eq. (13) (Section 3) in reference papers [4-6], is not valid for some cases like 8PSK and 16PSK modulations. The solution is done by finding a new alternative estimator  $M_{42}$ -NCCE in Eq. (19) (Section 4) for the mentioned digital modulation types (Section 2). The second problem, the performance of AMC in reference papers [4-8], worsens as the SNR value drops. The solution is using the most discriminative estimated HOCs through many steps: First, finding the mathematical forms of the estimated normalized HOMs (Section 5, Appendix 1) based on the estimated normalized coefficients. Second, finding the mathematical forms of the estimated normalized HOCs (Section 6, Appendix 2) based on the estimated HOMs. Finally, selecting the most

discriminative HOCs using features selection algorithms (Section 7). As a result, four estimated normalized HOCs have been selected (Section 7).

The selected HOCs could effectively improve classification accuracy compared with the reference papers [4-6]. The maximum ACC improvement compared with the reference paper [4] is 40.73%, compared with the reference paper [5] is 42.99, and compared with the reference paper [6] is 40.21%.

The classification accuracy is 100% for the case of three-tap multipath and SNR values greater than 6 dB (Section 8). In contrast, its classification accuracy is 100% for four-tap multipath and SNR values greater than 7 dB (Section 8).

## Abbreviations

AMC: Automatic Modulation Classification, HOMs: Higher-Order Moments, HOCs: Higher-Order Cumulants, MPSK: M-array Phase Shift Keying, MQAM: M-array quadrature amplitude shift modulation, SNR: Signal-to-noise ratio, AWGN: Additive white Gaussian noise, BPSK: binary phase-shift keying, QPSK: Quadrature Phase-Shift Keying, FSK: frequency-shift keying, CNN: convolutional neural network technique, PAM: Pulse-amplitude modulation, NCCE: Normalized channel coefficients estimator, ACC: classification accuracy.

## Appendix

### Appendix 1: The mathematical forms of the estimated HOMs

- 1) The mathematical form of  $\hat{M}_{40,x}$

$$\hat{M}_{40,x} = \frac{h(0)^{*2}}{h(0)^2} \left( \frac{\alpha_{40,0} M_{40,y}}{(M_{21,y} - N)^2} - 6\alpha_{40,1} \hat{m}_{20,x}^2 \right) := \frac{h(0)^{*2}}{h(0)^2} \hat{m}_{40,x},$$

$$\text{where } \alpha_{40} = \sum_{k=0}^{L-1} \hat{h}(k)^4, \alpha_{40,0} = \alpha_{21}^2 / \alpha_{40}, \alpha_{40,1} = \left( \sum_{k=0}^{L-2} \sum_{l=k+1}^{L-1} \hat{h}(k)^2 \hat{h}(l)^2 \right) / \alpha_{40}$$
(54)

, and  $M_{40,y}$  is a 4<sup>th</sup> order moment of the received signal.

- 2) The mathematical form of  $\hat{M}_{41,x}$

$$\hat{M}_{41,x} = \frac{h(0)^*}{h(0)} \left( \alpha_{41,0} \frac{(M_{41,y} - 3M_{20,y}N)}{(M_{21,y} - N)^2} - 3\alpha_{41,1} \hat{m}_{20,x} \hat{m}_{21,x} \right) := \frac{h(0)^*}{h(0)} \hat{m}_{41,x},$$

$$\text{where } \alpha_{41} = \sum_{k=0}^{L-1} \hat{h}(k)^3 \hat{h}(k)^*, \alpha_{41,0} = \alpha_{21}^2 / \alpha_{41}, \alpha_{41,1} = \left( \sum_{k=0}^{L-1} \sum_{l=0, l \neq k}^{L-1} \hat{h}(k)^2 |\hat{h}(l)|^2 \right) / \alpha_{41}$$
(55)

, and  $M_{41,y}$  is a 4<sup>th</sup> order moment of the received signal.

- 3) The mathematical form of  $\hat{M}_{42,x}$

$$\hat{M}_{42,x} = \alpha_{42,0} \frac{M_{42,y} - 4M_{21,y}N + 2N^2}{(M_{21,y} - N)^2} - 4\alpha_{42,1} \hat{m}_{21,x}^2 - \alpha_{42,2} |\hat{m}_{20,x}|^2 := \hat{m}_{42,x},$$

$$\text{where } \alpha_{42} = \sum_{k=0}^{L-1} |\hat{h}(k)|^4, \alpha_{42,0} = \alpha_{21}^2 / \alpha_{42}, \alpha_{42,1} = \left( \sum_{k=0}^{L-2} \sum_{l=k+1}^{L-1} |\hat{h}(k)|^2 |\hat{h}(l)|^2 \right) / \alpha_{42}$$

$$, \alpha_{42,2} = \left( \sum_{k=0}^{L-1} \sum_{l=0, l \neq k}^{L-1} \hat{h}(k)^2 \hat{h}(l)^{*2} \right) / \alpha_{42}$$
(56)

, and  $M_{42,y}$  is a 4<sup>th</sup> order moment of the received signal.

- 4) The mathematical form of  $\hat{M}_{60,x}$

$$\hat{M}_{60,x} = \frac{h(0)^{*3}}{h(0)^3} \left( \alpha_{60,0} \frac{M_{60,y}}{(M_{21,y} - N)^3} - 90\alpha_{60,1} \hat{m}_{20,x}^3 - 15\alpha_{60,2} \hat{m}_{40,x} \hat{m}_{20,x} \right) := \frac{h(0)^{*3}}{h(0)^3} \hat{m}_{60,x},$$

where  $\alpha_{60} = \sum_{k=0}^{L-1} \hat{h}(k)^6$ ,  $\alpha_{60,0} = \alpha_{21}^3 / \alpha_{60}$ ,  $\alpha_{60,1} = \left( \sum_{k=0}^{L-3} \sum_{l=k+1}^{L-2} \sum_{m=l+1}^{L-1} \hat{h}(k)^2 \hat{h}(l)^2 \hat{h}(m)^2 \right) / \alpha_{60}$

$$, \alpha_{60,2} = \left( \sum_{k=0}^{L-1} \sum_{l=0, l \neq k}^{L-1} \hat{h}(k)^4 \hat{h}(l)^2 \right) / \alpha_{60}$$
(57)

, and  $M_{60,y}$  is a 6<sup>th</sup> order moment of the received signal.

5) The mathematical form of  $\hat{M}_{61,x}$

$$\hat{M}_{61,x} = \frac{h(0)^{*2}}{h(0)^2} \left( \alpha_{61,0} \frac{M_{61,y} - 5M_{40,y}N}{(M_{21,y} - N)^3} - 5\alpha_{61,1} \hat{m}_{40,x} \hat{m}_{21,x} - 10\alpha_{61,2} \hat{m}_{40,x} \hat{m}_{21,x} \right) := \frac{h(0)^{*2}}{h(0)^2} \hat{m}_{61,x},$$

where  $\alpha_{61} = \sum_{k=0}^{L-1} \hat{h}(k)^5 \hat{h}(k)^*$ ,  $\alpha_{61,0} = \alpha_{21}^3 / \alpha_{61}$ ,  $\alpha_{61,1} = \left( \sum_{k=0}^{L-1} \sum_{l=0, l \neq k}^{L-1} \hat{h}(k)^4 |\hat{h}(l)|^2 \right) / \alpha_{61}$

$$, \alpha_{61,2} = \left( \sum_{k=0}^{L-1} \sum_{l=0, l \neq k}^{L-1} \hat{h}(k)^2 |\hat{h}(k)|^2 \hat{h}(l)^2 \right) / \alpha_{61}$$
(58)

, and  $M_{61,y}$  is a 6<sup>th</sup> order moment of the received signal.

6) The mathematical form of  $\hat{M}_{62,x}$

$$\hat{M}_{62,x} := \frac{h(0)^*}{h(0)} \left( \alpha_{62,0} \frac{M_{62,y} - 8M_{41,y}N + 12M_{20,y}N^2}{(M_{21,y} - N)^3} - 6\alpha_{62,1} \hat{m}_{42,x} \hat{m}_{20,x} - \alpha_{62,2} \hat{m}_{40,x} \hat{m}_{22,x} \right) := \frac{h(0)^*}{h(0)} \hat{m}_{62,x}$$

where  $\alpha_{62} = \sum_{k=0}^{L-1} \hat{h}(k)^4 \hat{h}(k)^{*2}$ ,  $\alpha_{62,0} = \alpha_{21}^3 / \alpha_{62}$ ,  $\alpha_{62,1} = \left( \sum_{k=0}^{L-2} \sum_{l=0, l \neq k}^{L-1} |\hat{h}(k)|^4 \hat{h}(l)^2 \right) / \alpha_{62}$

$$, \alpha_{62,2} = \left( \sum_{k=0}^{L-1} \sum_{l=0, l \neq k}^{L-1} \hat{h}(k)^4 \hat{h}(l)^{*2} \right) / \alpha_{62}, \alpha_{62,3} = \left( \sum_{k=0}^{L-1} \sum_{l=0, l \neq k}^{L-1} \hat{h}(k)^2 |\hat{h}(k)|^2 |\hat{h}(l)|^2 \right) / \alpha_{62}$$

$$, \alpha_{62,4} = \left( \sum_{k=0}^{L-1} \sum_{l=0, l \neq m}^{L-1} \sum_{m=l+1}^{L-1} |\hat{h}(k)|^2 |\hat{h}(l)|^2 \hat{h}(m)^2 \right) / \alpha_{62}, \alpha_{62,5} = \left( \sum_{k=0}^{L-1} \sum_{l=k+1}^{L-1} \sum_{m=0, m \neq k, l}^{L-1} \hat{h}(k)^2 \hat{h}(l)^2 \hat{h}(m)^{*2} \right) / \alpha_{62}$$
(59)

, and  $M_{62,y}$  is a 6<sup>th</sup> order moment of the received signal.

7) The mathematical form of  $\hat{M}_{63,x}$

$$\hat{M}_{63,x} = \alpha_{63,0} \frac{M_{63,y} - 9M_{42,y}N + 18M_{21,y}N^2}{(M_{21,y} - N)^3} - 9\alpha_{63,1} \hat{m}_{42,x} \hat{m}_{21,x} - 36\alpha_{63,2} \hat{m}_{21,x}^3$$

$$- 3\alpha_{63,3} \hat{m}_{41,x} \hat{m}_{22,x} - 9\alpha_{63,4} \hat{m}_{21,x} \hat{m}_{20,x} \hat{m}_{22,x} - 3\alpha_{63,5} \hat{m}_{43,x} \hat{m}_{20,x} := \hat{m}_{63,x}$$

where  $\alpha_{63} = \sum_{k=0}^{L-1} |\hat{h}(k)|^6$ ,  $\alpha_{63,0} = \alpha_{21}^3 / \alpha_{63}$ ,  $\alpha_{63,1} = \left( \sum_{k=0}^{L-1} \sum_{l=0, l \neq k}^{L-1} |\hat{h}(k)|^4 |\hat{h}(l)|^2 \right) / \alpha_{63}$

$$, \alpha_{63,2} = \left( \sum_{k=0}^{L-3} \sum_{l=k+1}^{L-2} \sum_{m=l+1}^{L-1} |\hat{h}(k)|^2 |\hat{h}(l)|^2 |\hat{h}(m)|^2 \right) / \alpha_{63}, \alpha_{63,3} = \left( \sum_{k=0}^{L-1} \sum_{l=0, l \neq k}^{L-1} \hat{h}(k)^2 |\hat{h}(k)|^2 \hat{h}(l)^{*2} \right) / \alpha_{63}$$

$$, \alpha_{63,4} = \left( \sum_{k=0}^{L-1} \sum_{l=0, l \neq k}^{L-1} \sum_{m=0, m \neq k}^{L-1} |\hat{h}(k)|^2 \hat{h}(l)^2 \hat{h}(m)^{*2} \right) / \alpha_{63}, \alpha_{63,5} = \left( \sum_{k=0}^{L-1} \sum_{l=0, l \neq k}^{L-1} \hat{h}(k)^{*2} |\hat{h}(k)|^2 \hat{h}(l)^2 \right) / \alpha_{63}$$
(60)

, and  $M_{63,y}$  is a 6<sup>th</sup> order moment of the received signal.

8) The mathematical form of  $\hat{M}_{80,x}$

$$\hat{M}_{80,x} = \frac{h(0)^{*4}}{h(0)^4} \left( \alpha_{80,0} \frac{M_{80,y}}{(M_{21,y} - N)^4} - 28\alpha_{80,1} \hat{m}_{60,x} \hat{m}_{20,x} - 70\alpha_{80,2} \hat{m}_{40,x}^2 \right) := \frac{h(0)^{*4}}{h(0)^4} \hat{m}_{80,x}$$

where  $\alpha_{80} = \sum_{k=0}^{L-1} \hat{h}(k)^8$ ,  $\alpha_{80,0} = \alpha_{21}^4 / \alpha_{80}$ ,  $\alpha_{80,1} = \left( \sum_{k=0}^{L-1} \sum_{l=0, l \neq k}^{L-1} \hat{h}(k)^6 \hat{h}(l)^2 \right) / \alpha_{80}$

$$, \alpha_{80,2} = \left( \sum_{k=0}^{L-2} \sum_{l=k+1}^{L-1} \hat{h}(k)^4 \hat{h}(l)^4 \right) / \alpha_{80}, \alpha_{80,3} = \left( \sum_{k=0}^{L-1} \sum_{l=0, l \neq k}^{L-2} \sum_{m=l+1}^{L-1} \hat{h}(k)^4 \hat{h}(l)^2 \hat{h}(m)^2 \right) / \alpha_{80}$$

$$, \alpha_{80,4} = \left( \sum_{k=0}^{L-4} \sum_{l=k+1}^{L-3} \sum_{m=l+1}^{L-2} \sum_{t=m+1}^{L-1} \hat{h}(k)^2 \hat{h}(l)^2 \hat{h}(m)^2 \hat{h}(t)^2 \right) / \alpha_{80}$$
(61)

, and  $M_{80,y}$  is a 8<sup>th</sup> order moment of the received signal.

9) The mathematical form of  $\hat{M}_{81,x}$

$$\hat{M}_{81,x} = \frac{h(0)^{*3}}{h(0)^3} \left( \alpha_{81,0} \frac{M_{81,y} - 7M_{60,y}N}{(M_{21,y} - N)^4} - 7\alpha_{81,1} \hat{m}_{60,x} \hat{m}_{21,x} - 21\alpha_{81,2} \hat{m}_{61,x} \hat{m}_{20,x} - 35\alpha_{81,3} \hat{m}_{40,x} \hat{m}_{41,x} \right) := \frac{h(0)^{*3}}{h(0)^3} \hat{m}_{81,x}$$

where  $\alpha_{81} = \sum_{k=0}^{L-1} \hat{h}(k)^7 \hat{h}(k)^*$ ,  $\alpha_{81,0} = \alpha_{21}^4 / \alpha_{81}$ ,  $\alpha_{81,1} = \left( \sum_{k=0}^{L-1} \sum_{l=0, l \neq k}^{L-1} \hat{h}(k)^6 |\hat{h}(l)|^2 \right) / \alpha_{81}$

$$, \alpha_{81,2} = \left( \sum_{k=0}^{L-1} \sum_{l=0, l \neq k}^{L-1} \hat{h}(k)^4 |\hat{h}(k)|^2 \hat{h}(l)^2 \right) / \alpha_{81}, \alpha_{81,3} = \left( \sum_{k=0}^{L-1} \sum_{l=0, l \neq k}^{L-1} \hat{h}(k)^4 \hat{h}(l)^2 |\hat{h}(l)|^2 \right) / \alpha_{81}$$

$$, \alpha_{81,4} = \left( \sum_{k=0}^{L-1} \sum_{l=0, l \neq k}^{L-1} \sum_{m=0, m \neq l, k}^{L-1} \hat{h}(k)^4 \hat{h}(l)^2 |\hat{h}(m)|^2 \right) / \alpha_{81}$$

$$, \alpha_{81,5} = \left( \sum_{k=0}^{L-1} \sum_{l=0, l \neq k}^{L-2} \sum_{m=l+1}^{L-1} \hat{h}(k)^2 |\hat{h}(k)|^2 \hat{h}(l)^2 \hat{h}(m)^2 \right) / \alpha_{81}$$

$$, \alpha_{81,6} = \left( \sum_{k=0}^{L-3} \sum_{l=k+1}^{L-2} \sum_{m=l+1}^{L-1} \sum_{t=1, t \neq k, l, m}^{L-1} |\hat{h}(k)|^2 \hat{h}(l)^2 \hat{h}(m)^2 \hat{h}(t)^2 \right) / \alpha_{81}$$
(62)

, and  $M_{81,y}$  is a 8<sup>th</sup> order moment of the received signal.

10) The mathematical form of  $\hat{M}_{82,x}$

$$\hat{M}_{82,x} = \frac{h(0)^{*2}}{h(0)^2} \left( \begin{array}{l} \alpha_{82,0} \frac{M_{82,y} - 13M_{61,y}N + 34M_{40,y}N^2}{(M_{21,y} - N)^4} - 15\alpha_{82,1}\hat{m}_{40,x}\hat{m}_{42,x} - \alpha_{82,2}\hat{m}_{60,x}\hat{m}_{22,x} \\ -12\alpha_{82,3}\hat{m}_{61,x}\hat{m}_{21,x} - 60\alpha_{82,4}\hat{m}_{40,x}\hat{m}_{21,x}^2 - 15\alpha_{82,5}\hat{m}_{62,x}\hat{m}_{20,x} - 15\alpha_{82,6}\hat{m}_{40,x}\hat{m}_{20,x}\hat{m}_{22,x} \\ -90\alpha_{82,7}\hat{m}_{42,x}\hat{m}_{20,x}^2 - 90\alpha_{82,8}\hat{m}_{22,x}\hat{m}_{20,x}^3 - 40\alpha_{82,8}\hat{m}_{41,x}^2 - 120\alpha_{82,9}\hat{m}_{41,x}\hat{m}_{21,x}\hat{m}_{20,x} \\ -360\alpha_{82,10}\hat{m}_{21,x}^2\hat{m}_{20,x}^2 \end{array} \right) := \frac{h(0)^{*2}}{h(0)^2} \hat{m}_{82,x}$$

where  $\alpha_{82} = \sum_{k=0}^{L-1} \hat{h}(k)^6 \hat{h}(k)^{*2}$ ,  $\alpha_{82,0} = \alpha_{21}^4 / \alpha_{82}$ ,  $\alpha_{82,1} = \left( \sum_{k=0}^{L-1} \sum_{l=0, l \neq k}^{L-1} \hat{h}(k)^4 |\hat{h}(l)|^4 \right) / \alpha_{82}$

,  $\alpha_{82,2} = \left( \sum_{k=0}^{L-1} \sum_{l=0, l \neq k}^{L-1} \hat{h}(k)^6 \hat{h}(l)^{*2} \right) / \alpha_{82}$ ,  $\alpha_{82,3} = \left( \sum_{k=0}^{L-1} \sum_{l=0, l \neq k}^{L-1} \hat{h}(k)^4 |\hat{h}(k)|^2 |\hat{h}(l)|^2 \right) / \alpha_{82}$

,  $\alpha_{82,4} = \left( \sum_{k=0}^{L-1} \sum_{l=0, l \neq k}^{L-2} \sum_{m=l+1}^{L-1} \hat{h}(k)^4 |\hat{h}(l)|^2 |\hat{h}(m)|^2 \right) / \alpha_{82}$ ,  $\alpha_{82,5} = \left( \sum_{k=0}^{L-1} \sum_{l=0, l \neq k}^{L-1} \hat{h}(k)^4 \hat{h}(k)^{*2} \hat{h}(l)^2 \right) / \alpha_{82}$

,  $\alpha_{82,6} = \left( \sum_{k=0}^{L-1} \sum_{l=0, l \neq k}^{L-1} \sum_{m=0, m \neq k, l}^{L-1} \hat{h}(k)^4 \hat{h}(l)^2 \hat{h}(m)^{*2} \right) / \alpha_{82}$ ,  $\alpha_{82,7} = \left( \sum_{k=0}^{L-1} \sum_{l=0, l \neq k}^{L-2} \sum_{m=l+1}^{L-1} |\hat{h}(k)|^4 \hat{h}(l)^2 \hat{h}(m)^2 \right) / \alpha_{82}$

,  $\alpha_{82,8} = \left( \sum_{k=0}^{L-1} \sum_{l=1, l \neq k}^{L-2} \sum_{m=l+1, m \neq k, l}^{L-1} \sum_{t=m+1, t \neq k, l, m}^{L-1} \hat{h}(k)^{*2} \hat{h}(l)^2 \hat{h}(m)^2 \hat{h}(t)^2 \right) / \alpha_{82}$

,  $\alpha_{82,8} = \left( \sum_{k=0}^{L-2} \sum_{m=l+1}^{L-1} \hat{h}(k)^2 |\hat{h}(k)|^2 \hat{h}(l)^2 |\hat{h}(l)|^2 \right) / \alpha_{82}$

,  $\alpha_{82,9} = \left( \sum_{k=0}^{L-1} \sum_{l=0, l \neq k}^{L-1} \sum_{m=1, m \neq k, l}^{L-1} \hat{h}(k)^2 |\hat{h}(k)|^2 |\hat{h}(l)|^2 \hat{h}(m)^2 \right) / \alpha_{82}$

,  $\alpha_{82,10} = \left( \sum_{k=0}^{L-2} \sum_{l=k+1}^{L-1} \sum_{m=1, m \neq k, l}^{L-2} \sum_{t=m+1}^{L-1} |\hat{h}(k)|^2 |\hat{h}(l)|^2 \hat{h}(m)^2 \hat{h}(t)^2 \right) / \alpha_{82}$

, and  $M_{82,y}$  is a 8<sup>th</sup> order moment of the received signal.

11) The mathematical form of  $\hat{M}_{83,x}$

(64)

$$\hat{M}_{83,x} = \frac{h(0)^*}{h(0)} \left( \begin{array}{l} \alpha_{83,0} \frac{M_{83,y} - 15M_{62,y}N + 60M_{41,y}N^2 - 60M_{20,y}N^3}{(M_{21,y} - N)^4} - 10\alpha_{83,1}\hat{m}_{63,x}\hat{m}_{20,x} \\ -3\alpha_{83,2}\hat{m}_{61,x}\hat{m}_{22,x} - 5\alpha_{83,3}\hat{m}_{40,x}\hat{m}_{43,x} - 30\alpha_{83,4}\hat{m}_{42,x}\hat{m}_{41,x} - 30\alpha_{83,5}\hat{m}_{41,x}\hat{m}_{20,x}\hat{m}_{22,x} \\ -30\alpha_{83,6}\hat{m}_{43,x}\hat{m}_{20,x}^2 - 15\alpha_{83,7}\hat{m}_{62,x}\hat{m}_{21,x} - 15\alpha_{83,8}\hat{m}_{40,x}\hat{m}_{21,x}\hat{m}_{22,x} \\ -90\alpha_{83,9}\hat{m}_{21,x}\hat{m}_{22,x}\hat{m}_{20,x}^2 - 90\alpha_{83,10}\hat{m}_{42,x}\hat{m}_{21,x}\hat{m}_{20,x} - 120\alpha_{83,11}\hat{m}_{41,x}\hat{m}_{21,x}^2 \\ -360\alpha_{83,12}\hat{m}_{20,x}\hat{m}_{21,x}^3 \end{array} \right) := \frac{h(0)^*}{h(0)} \hat{m}_{83,x}$$

where  $\alpha_{83} = \sum_{k=0}^{L-1} \hat{h}(k)^5 \hat{h}(k)^{*3}$ ,  $\alpha_{83,0} = \alpha_{21}^4 / \alpha_{83}$ ,  $\alpha_{83,1} = \left( \sum_{k=0}^{L-1} \sum_{l=0, l \neq k}^{L-1} \hat{h}(k)^3 \hat{h}(k)^{*3} \hat{h}(l)^2 \right) / \alpha_{83}$

$\alpha_{83,2} = \left( \sum_{k=0}^{L-1} \sum_{l=0, l \neq k}^{L-1} \hat{h}(k)^5 \hat{h}(k)^* \hat{h}(l)^{*2} \right) / \alpha_{83}$ ,  $\alpha_{83,3} = \left( \sum_{k=0}^{L-1} \sum_{l=0, l \neq k}^{L-1} \hat{h}(k)^4 \hat{h}(l) \hat{h}(l)^{*3} \right) / \alpha_{83}$

$\alpha_{83,4} = \left( \sum_{k=0}^{L-1} \sum_{l=0, l \neq k}^{L-1} |\hat{h}(k)|^4 \hat{h}(l)^3 \hat{h}(l)^* \right) / \alpha_{83}$ ,  $\alpha_{83,5} = \left( \sum_{k=0}^{L-1} \sum_{l=0, l \neq k}^{L-1} \sum_{m=0, m \neq k, l}^{L-1} \hat{h}(k)^3 \hat{h}(k)^* \hat{h}(l)^2 \hat{h}(l)^{*2} \right) / \alpha_{83}$

$\alpha_{83,6} = \left( \sum_{k=0}^{L-1} \sum_{l=0, l \neq k}^{L-2} \sum_{m=l+1}^{L-1} \hat{h}(k) \hat{h}(k)^{*3} \hat{h}(l)^2 \hat{h}(m)^2 \right) / \alpha_{83}$ ,  $\alpha_{83,7} = \left( \sum_{k=0}^{L-1} \sum_{l=0, l \neq k}^{L-1} \hat{h}(k)^4 \hat{h}(k)^{*2} |\hat{h}(l)|^2 \right) / \alpha_{83}$

$\alpha_{83,8} = \left( \sum_{k=0}^{L-1} \sum_{l=0, l \neq k}^{L-1} \sum_{m=0, m \neq k, l}^{L-1} \hat{h}(k)^4 |\hat{h}(l)|^2 \hat{h}(m)^{*2} \right) / \alpha_{83}$

$\alpha_{83,9} = \left( \sum_{k=0}^{L-1} \sum_{l=1, l \neq k}^{L-2} \sum_{m=l+1}^{L-1} \sum_{t=1, t \neq k, l, m}^{L-1} |\hat{h}(k)|^2 \hat{h}(l)^2 \hat{h}(m)^2 \hat{h}(t)^{*2} \right) / \alpha_{83}$

$\alpha_{83,10} = \left( \sum_{k=0}^{L-1} \sum_{l=0, l \neq k}^{L-1} \sum_{m=0, m \neq k, l}^{L-1} |\hat{h}(k)|^4 |\hat{h}(l)|^2 \hat{h}(m)^2 \right) / \alpha_{83}$

$\alpha_{83,11} = \left( \sum_{k=0}^{L-1} \sum_{l=0, l \neq k}^{L-1} \sum_{m=l+1}^{L-1} \hat{h}(k)^2 |\hat{h}(k)|^2 |\hat{h}(l)|^2 |\hat{h}(m)|^2 \right) / \alpha_{83}$

$\alpha_{83,12} = \left( \sum_{k=0}^{L-3} \sum_{l=k+1}^{L-2} \sum_{m=l+1}^{L-1} \sum_{t=1, t \neq k, l, m}^{L-1} |\hat{h}(k)|^2 |\hat{h}(l)|^2 |\hat{h}(m)|^2 \hat{h}(t)^2 \right) / \alpha_{83}$

, and  $M_{83,y}$  is a 8<sup>th</sup> order moment of the received signal.

12) The mathematical form of  $\hat{M}_{84,x}$

$$\begin{aligned}
\hat{M}_{84,x} = & \alpha_{84,0} \frac{M_{84,y} - 16M_{63,y}N + 72M_{42,y}N^2 - 96M_{21,y}N^3 - 72N^4}{(M_{21,y} - N)^4} - \alpha_{84,1}\hat{m}_{40,x}\hat{m}_{44,x} - 6\alpha_{84,2}\hat{m}_{62,x}\hat{m}_{22,x} \\
& - 6\alpha_{84,3}\hat{m}_{40,x}\hat{m}_{22,x}^2 - 6\alpha_{84,4}\hat{m}_{64,x}\hat{m}_{20,x} - 6\alpha_{84,5}\hat{m}_{44,x}\hat{m}_{20,x}^2 - 16\alpha_{84,6}\hat{m}_{63,x}\hat{m}_{21,x} - 16\alpha_{84,7}\hat{m}_{41,x}\hat{m}_{43,x} \\
& - 36\alpha_{84,8}\hat{m}_{42,x}^2 - 36\alpha_{84,9}\hat{m}_{42,x}\hat{m}_{20,x}\hat{m}_{22,x} - 36\alpha_{84,10}\hat{m}_{20,x}^2\hat{m}_{22,x} - 48\alpha_{84,11}\hat{m}_{43,x}\hat{m}_{21,x}\hat{m}_{20,x} \\
& - 48\alpha_{84,12}\hat{m}_{41,x}\hat{m}_{21,x}\hat{m}_{22,x} - 144\alpha_{84,13}\hat{m}_{42,x}\hat{m}_{21,x}^2 - 144\alpha_{84,14}\hat{m}_{21,x}^2\hat{m}_{20,x}\hat{m}_{22,x} - 576\alpha_{84,15}\hat{m}_{21,x}^4 := \hat{m}_{84,x} \\
\text{where } \alpha_{84} = & \sum_{k=0}^{L-1} |\hat{h}(k)|^8, \alpha_{84,0} = \alpha_{21}^4 / \alpha_{84}, \alpha_{84,1} = \left( \sum_{k=0}^{L-1} \sum_{l=0, l \neq k}^{L-1} \hat{h}(k)^4 \hat{h}(l)^4 \right) / \alpha_{84} \\
, \alpha_{84,2} = & \left( \sum_{k=0}^{L-1} \sum_{l=0, l \neq k}^{L-1} \hat{h}(k)^4 \hat{h}(k)^* \hat{h}(l)^* \hat{h}(l)^2 \right) / \alpha_{84}, \alpha_{84,3} = \left( \sum_{k=0}^{L-1} \sum_{l=0, l \neq k}^{L-1} \sum_{m=l+1}^{L-1} \hat{h}(k)^4 \hat{h}(l)^* \hat{h}(m)^* \right) / \alpha_{84} \\
, \alpha_{84,4} = & \left( \sum_{k=0}^{L-1} \sum_{l=0, l \neq k}^{L-1} \hat{h}(k)^* \hat{h}(k)^2 \hat{h}(l)^2 \right) / \alpha_{84}, \alpha_{84,5} = \left( \sum_{k=0}^{L-1} \sum_{l=0, l \neq k}^{L-2} \sum_{m=l+1}^{L-1} \hat{h}(k)^* \hat{h}(l)^2 \hat{h}(m)^2 \right) / \alpha_{84} \\
, \alpha_{84,6} = & \sum_{k=0}^{L-1} \sum_{l=0, l \neq k}^{L-1} |\hat{h}(k)|^6 \hat{h}(l)^* \hat{h}(l)^2 / \alpha_{84}, \alpha_{84,7} = \left( \sum_{k=0}^{L-1} \sum_{l=0, l \neq k}^{L-1} \hat{h}(k)^2 |\hat{h}(k)|^2 \hat{h}(l)^* \hat{h}(l)^2 \right) / \alpha_{84} \\
, \alpha_{84,8} = & \left( \sum_{k=0}^{L-2} \sum_{l=k+1}^{L-1} |\hat{h}(k)|^4 |\hat{h}(l)|^4 \right) / \alpha_{84}, \alpha_{84,9} = \left( \sum_{k=0}^{L-1} \sum_{l=0, l \neq k}^{L-1} \sum_{m=1, m \neq k, l}^{L-1} |\hat{h}(k)|^4 \hat{h}(l)^2 \hat{h}(m)^* \right) / \alpha_{84} \\
, \alpha_{84,10} = & \left( \sum_{k=0}^{L-2} \sum_{l=k+1}^{L-1} \sum_{m=1}^{L-1} \sum_{t=m+1, t \neq k, l}^{L-1} \hat{h}(k)^2 \hat{h}(l)^2 \hat{h}(m)^* \hat{h}(t)^* \right) / \alpha_{84} \\
, \alpha_{84,11} = & \left( \sum_{k=0}^{L-1} \sum_{l=0, l \neq k}^{L-1} \sum_{m=1, m \neq k, l}^{L-1} \hat{h}(k)^* \hat{h}(k) |\hat{h}(l)|^2 \hat{h}(m)^2 \right) / \alpha_{84} \\
, \alpha_{84,12} = & \left( \sum_{k=0}^{L-1} \sum_{l=0, l \neq k}^{L-1} \sum_{m=1, m \neq k, l}^{L-1} \hat{h}(k)^3 \hat{h}(k)^* |\hat{h}(l)|^2 \hat{h}(m)^* \right) / \alpha_{84} \\
, \alpha_{84,13} = & \left( \sum_{k=0}^{L-1} \sum_{l=0, l \neq k}^{L-2} \sum_{m=l+1, m \neq k}^{L-1} |\hat{h}(k)|^4 |\hat{h}(l)|^2 |\hat{h}(m)|^2 \right) / \alpha_{84} \\
, \alpha_{84,14} = & \left( \sum_{k=0}^{L-2} \sum_{l=k+1}^{L-1} \sum_{m=1}^{L-1} \sum_{t=1, t \neq k, l}^{L-1} |\hat{h}(k)|^2 |\hat{h}(l)|^2 \hat{h}(m)^2 \hat{h}(t)^* \right) / \alpha_{84} \\
, \alpha_{84,15} = & \left( \sum_{k=0}^{L-4} \sum_{l=k+1}^{L-3} \sum_{m=l+1}^{L-2} \sum_{t=m+1}^{L-1} |\hat{h}(k)|^2 |\hat{h}(l)|^2 |\hat{h}(m)|^2 |\hat{h}(t)|^2 \right) / \alpha_{84}
\end{aligned} \tag{65}$$

, and  $M_{84,y}$  is a 8<sup>th</sup> order moment of the received signal.

## Appendix 2: The mathematical forms of the estimated HOCs

- 1) The mathematical form of  $\hat{C}_{41,x}$

$$\hat{C}_{41,x} := \frac{h(0)^*}{h(0)} (\hat{m}_{41} - 3\hat{m}_{20}\hat{m}_{21}) := \frac{h(0)^*}{h(0)} \hat{c}_{41,x} \tag{66}$$

- 2) The mathematical form of  $\hat{C}_{42,x}$

$$\hat{C}_{42,x} := \hat{m}_{42} - |\hat{m}_{20}|^2 - 2\hat{m}_{21}^2 := \hat{c}_{42,x} \tag{67}$$

- 3) The mathematical form of  $\hat{C}_{60,x}$

$$\hat{C}_{60,x} := \frac{h(0)^*{}^3}{h(0)^3} (\hat{m}_{60} - 15\hat{m}_{20}\hat{m}_{40} + 30\hat{m}_{20}^3) := \frac{h(0)^*{}^3}{h(0)^3} \hat{c}_{60,x} \tag{68}$$

- 4) The mathematical form of  $\hat{C}_{61,x}$



$$\hat{C}_{61,x} := \frac{h(0)^{*2}}{h(0)^2} (\hat{m}_{61} - 5\hat{m}_{21}\hat{m}_{40} - 10\hat{m}_{20}\hat{m}_{41} + 30\hat{m}_{20}^2\hat{m}_{21}) := \frac{h(0)^{*2}}{h(0)^2} \hat{c}_{61,x} \quad (69)$$

5) The mathematical form of  $\hat{C}_{62,x}$

$$\hat{C}_{62,x} = \frac{h(0)^{*}}{h(0)} (\hat{m}_{62} - 6\hat{m}_{20}\hat{m}_{42} - 8\hat{m}_{21}\hat{m}_{41} - \hat{m}_{22}\hat{m}_{40} + 6\hat{m}_{20}^2\hat{m}_{22} + 24\hat{m}_{21}^2\hat{m}_{22}) := \frac{h(0)^{*}}{h(0)} \hat{c}_{62,x} \quad (70)$$

6) The mathematical form of  $\hat{C}_{63,x}$

$$\hat{C}_{63,x} = \hat{m}_{63} - 9\hat{m}_{21}\hat{m}_{42} + 12\hat{m}_{21}^3 - 3\hat{m}_{20}\hat{m}_{43} - 3\hat{m}_{22}\hat{m}_{41} + 18\hat{m}_{20}\hat{m}_{21}\hat{m}_{22} := \hat{c}_{63,x} \quad (71)$$

7) The mathematical form of  $\hat{C}_{80,x}$

$$\hat{C}_{80,x} = \frac{h(0)^{*4}}{h(0)^4} (\hat{m}_{80} - 35\hat{m}_{40}^2 - 28\hat{m}_{60}\hat{m}_{20} + 420\hat{m}_{20}^2\hat{m}_{40} - 630\hat{m}_{20}^4) := \frac{h(0)^{*4}}{h(0)^4} \hat{c}_{80,x} \quad (72)$$

8) The mathematical form of  $\hat{C}_{81,x}$

$$\begin{aligned} \hat{C}_{81,x} &= \frac{h(0)^{*3}}{h(0)^3} (\hat{m}_{81} - 7\hat{m}_{60}\hat{m}_{21} - 21\hat{m}_{61}\hat{m}_{20} - 35\hat{m}_{40}\hat{m}_{41} + 210\hat{m}_{40}\hat{m}_{20}\hat{m}_{21} + 210\hat{m}_{20}^2\hat{m}_{41} - 630\hat{m}_{20}^3\hat{m}_{21}) \\ &:= \frac{h(0)^{*3}}{h(0)^3} \hat{c}_{81,x} \end{aligned} \quad (73)$$

9) The mathematical form of  $\hat{C}_{82,x}$

$$\begin{aligned} \hat{C}_{82,x} &= \frac{h(0)^{*2}}{h(0)^2} \left( \hat{m}_{82} - \hat{m}_{60}\hat{m}_{22} - 12\hat{m}_{61}\hat{m}_{21} - 15\hat{m}_{62}\hat{m}_{20} - 15\hat{m}_{40}\hat{m}_{42} + 30\hat{m}_{40}\hat{m}_{20}\hat{m}_{22} + 60\hat{m}_{40}\hat{m}_{21}^2 \right. \\ &\quad \left. - 20\hat{m}_{41}^2 + 240\hat{m}_{41}\hat{m}_{20}\hat{m}_{21} + 90\hat{m}_{42}\hat{m}_{20}^2 - 90\hat{m}_{20}^3\hat{m}_{22} - 540\hat{m}_{20}^2\hat{m}_{21}^2 \right) \\ &:= \frac{h(0)^{*2}}{h(0)^2} \hat{c}_{82,x} \end{aligned} \quad (74)$$

10) The mathematical form of  $\hat{C}_{83,x}$

$$\begin{aligned} \hat{C}_{83,x} &= \frac{h(0)^{*}}{h(0)} \left( \hat{m}_{83} - 3\hat{m}_{61}\hat{m}_{22} - 15\hat{m}_{62}\hat{m}_{21} - 5\hat{m}_{40}\hat{m}_{43} + 30\hat{m}_{40}\hat{m}_{21}\hat{m}_{22} - 10\hat{m}_{63}\hat{m}_{20} - 30\hat{m}_{41}\hat{m}_{42} \right. \\ &\quad \left. + 60\hat{m}_{41}\hat{m}_{20}\hat{m}_{22} + 120\hat{m}_{41}\hat{m}_{21}^2 + 30\hat{m}_{20}^2\hat{m}_{43} - 270\hat{m}_{20}^2\hat{m}_{21}\hat{m}_{22} - 360\hat{m}_{20}\hat{m}_{21}^3 + 180\hat{m}_{20}\hat{m}_{42}\hat{m}_{21} \right) \\ &:= \frac{h(0)^{*}}{h(0)} \hat{c}_{83,x} \end{aligned} \quad (75)$$

11) The mathematical form of  $\hat{C}_{84,x}$

$$\hat{C}_{84,x} = \hat{m}_{84} - 16\hat{c}_{63}\hat{c}_{21} + |\hat{c}_{40}|^2 - 18\hat{c}_{42}^2 - 72\hat{c}_{42}\hat{c}_{21}^2 - 24\hat{c}_{21}^4 := \hat{c}_{84,x} \quad (76)$$

## Funding

No funds, grants, or other support was received.

## Conflict of interest

The authors declare that they have no conflict of interest.

## Data Availability

Data sharing does not apply to this article as random signals were generated or analyzed during the current study.

## Code availability

The code supporting the current study have not been deposited in a public repository because is part of an on-going research.

## Authors contributions

Iyad Kadoun and Hossein Khaleghi Bizaki proposed the main idea of the innovation of the paper. Iyad Kadoun performed the simulations, carried out the data analysis, interpreted the results and wrote the manuscript. Iyad Kadoun and Hossein Khaleghi Bizaki corrected the proofing the article.

## References

1. Bany Muhammad, N., Ghauri, S., Sarfraz, M., & Masood, S. (2021). Optimized Polynomial Classifier for Classification of M-PSK signals. <https://doi.org/10.18280/mmep.080410>.
2. Han, H., Ren, Z., Li, L., & Zhu, Z. J. S. (2021). Automatic Modulation Classification Based on Deep Feature Fusion for High Noise Level and Large Dynamic Input. *21*(6), 2117. <https://doi.org/10.3390/s21062117>.
3. SIMIC, M., STANKOVIC, M., & ORLIC, V. D. J. R. (2021). Automatic Modulation Classification of Real Signals in AWGN Channel Based on Sixth-Order Cumulants. *30*(1). <https://doi.org/10.13164/re.2021.0204>.
4. Wu, H.-C., Saquib, M., & Yun, Z. J. I. T. o. W. C. (2008). Novel automatic modulation classification using cumulant features for communications via multipath channels. *7*(8), 3098-3105. <https://doi.org/10.1109/TWC.2008.070015>.
5. Orlic, V. D., & Dukic, M. L. J. I. C. L. (2009). Automatic modulation classification algorithm using higher-order cumulants under real-world channel conditions. *13*(12), 917-919. <https://doi.org/10.1109/LCOMM.2009.12.091711>.
6. Chang, D.-C., & Shih, P.-K. J. I. C. (2015). Cumulants-based modulation classification technique in multipath fading channels. *9*(6), 828-835. <https://doi.org/10.1049/iet-com.2014.0773>.
7. Tekbıyık, K., Ekti, A. R., Görçin, A., Kurt, G. K., & Keçeci, C. (2020). Robust and fast automatic modulation classification with CNN under multipath fading channels. 2020 IEEE 91st Vehicular Technology Conference (VTC2020-Spring), <https://doi.org/10.1109/VTC2020-Spring48590.2020.9128408>.
8. Zhang, Z., Hua, Z., & Liu, Y. J. I. c. (2017). Modulation classification in multipath fading channels using sixth-order cumulants and stacked convolutional auto-encoders. *11*(6), 910-915. <https://doi.org/10.1049/ietcom.2016.0533>.
9. El-Khamy, S. E., & Elsayed, H. A. (2012). Classification of multi-user chirp modulation signals using wavelet higher-order-statistics features and artificial intelligence techniques. *Int'l J. of Communications, Network and System Sciences*, *5*(09), 520. <https://doi.org/10.4236/ijcns.2012.59063>.
10. Bozovic, R., & Simic, M. (2019). Spectrum Sensing Based on Higher Order Cumulants and Kurtosis Statistics Tests in Cognitive Radio. *Radioengineering*, *29*(2). <https://doi.org/10.13164/re.2019.0464>.
11. Abdelmutalab, A. E. (2015). *Learning-based automatic modulation classification*
12. Abdelmutalab, A., Assaleh, K., & El-Tarhuni, M. J. P. C. (2016). Automatic modulation classification based on high order cumulants and hierarchical polynomial classifiers. *21*, 10-18. <https://doi.org/10.1016/j.phycom.2016.08.001>.
13. Sekhar, S. C., & Sreenivas, T. J. S. P. (2006). Signal-to-noise ratio estimation using higher-order moments. *86*(4), 716-732. <https://doi.org/10.1016/j.sigpro.2005.06.003>.
14. Dobre, O. A., Abdi, A., Bar-Ness, Y., & Su, W. J. I. c. (2007). Survey of automatic modulation classification techniques: classical approaches and new trends. *1*(2), 137-156. <https://doi.org/10.1049/iet-com:20050176>.
15. Ghauri, S. A., Qureshi, I. M., Aziz, A., & Cheema, T. A. J. W. A. S. J. (2014). Classification of digital modulated signals using linear discriminant analysis on faded channel. *29*(10), 1220-1227. <https://doi.org/10.5829/idosi.wasj.2014.29.10.1540>.
16. Ali, A. K., & Erçelebi, E. (2019). An M-QAM signal modulation recognition algorithm in AWGN channel. *Scientific Programming*, 2019. <https://doi.org/10.1155/2019/6752694>.
17. Ghauri, S. A., Qureshi, I. M., Malik, A. N., & Cheema, T. A. (2013). Higher order cummulants based digital modulation recognition scheme. *Research Journal of Applied Sciences Engineering & Technology*, *6*(20), 3910-3915. <https://doi.org/10.19026/rjaset.6.3609>.
18. Mühlhaus, M. S. (2014). *Automatische Modulationsartenerkennung in MIMO-Systemen* Inst. für Nachrichtentechnik].
19. Abdelbar, M., Tranter, W. H., Bose, T. J. I. T. o. C. C., & Networking. (2018). Cooperative cumulants-based modulation classification in distributed networks. *4*(3), 446-461. <https://doi.org/10.19026/rjaset.6.3609>.

20. KADOUN, I., & BIZAKI, H. K. J. R. (2022). Advanced Features Generation Algorithm for MPSK and MQAM Classification in Flat Fading Channel. *31*(1), 127. <https://doi.org/10.13164/re.2022.0127>.
21. Li, J., Cheng, K., Wang, S., Morstatter, F., Trevino, R. P., Tang, J., & Liu, H. (2017). Feature selection: A data perspective. *ACM Computing Surveys (CSUR)*, *50*(6), 1-45.
22. Eid, H. F., Hassanien, A. E., Kim, T.-h., & Banerjee, S. (2013). Linear correlation-based feature selection for network intrusion detection model. International Conference on Security of Information and Communication Networks, [https://doi.org/10.1007/978-3-642-40597-6\\_21](https://doi.org/10.1007/978-3-642-40597-6_21).

#### ORCID

Iyad Kadoun  <https://orcid.org/0000-0003-1999-6066>.

Hossein Khaleghi Bizaki  <https://orcid.org/0000-0001-9458-8287>.